Title: Probes of cosmic inflation: from the CMB to quantum systems

Speakers: Emilie Hertig

Collection/Series: Cosmology and Gravitation

Subject: Cosmology

Date: December 12, 2024 - 11:00 AM

URL: https://pirsa.org/24120027

Abstract:

Polarization anisotropies of the cosmic microwave background (CMB) encode a wealth of information on fundamental physics. In the coming decade, a new generation of instruments starting with the Simons Observatory (SO) will either detect or tightly constrain the amplitude of B-mode patterns produced by inflationary gravitational waves. The first part of my talk will focus on techniques developed to mitigate secondary B-modes induced by Galactic foregrounds and weak gravitational lensing, in order to extract the primordial signal with optimal precision. I will present resulting performance forecasts for SO, as well as initial efforts to apply these methods to the new data currently being collected.

At the other end of the scale, complementary approaches based on numerical simulations and cold-atom analogue experiments are emerging as a way of probing early-Universe quantum dynamics in real time. The second part of my talk will introduce ongoing work on lattice simulations of false vacuum decay, aiming to understand their range of validity by investigating renormalization effects. Finally, I will outline future avenues for combining cosmological and quantum probes of inflation, exploiting the deep connection between the smallest and largest scales to gain a new perspective on the early Universe.

Probes of Cosmic Inflation

From the CMB to quantum systems

Emilie Hertig

With A. Challinor, B. Sherwin,
H. Peiris *et al.*

Perimeter Institute, 12.12.2024

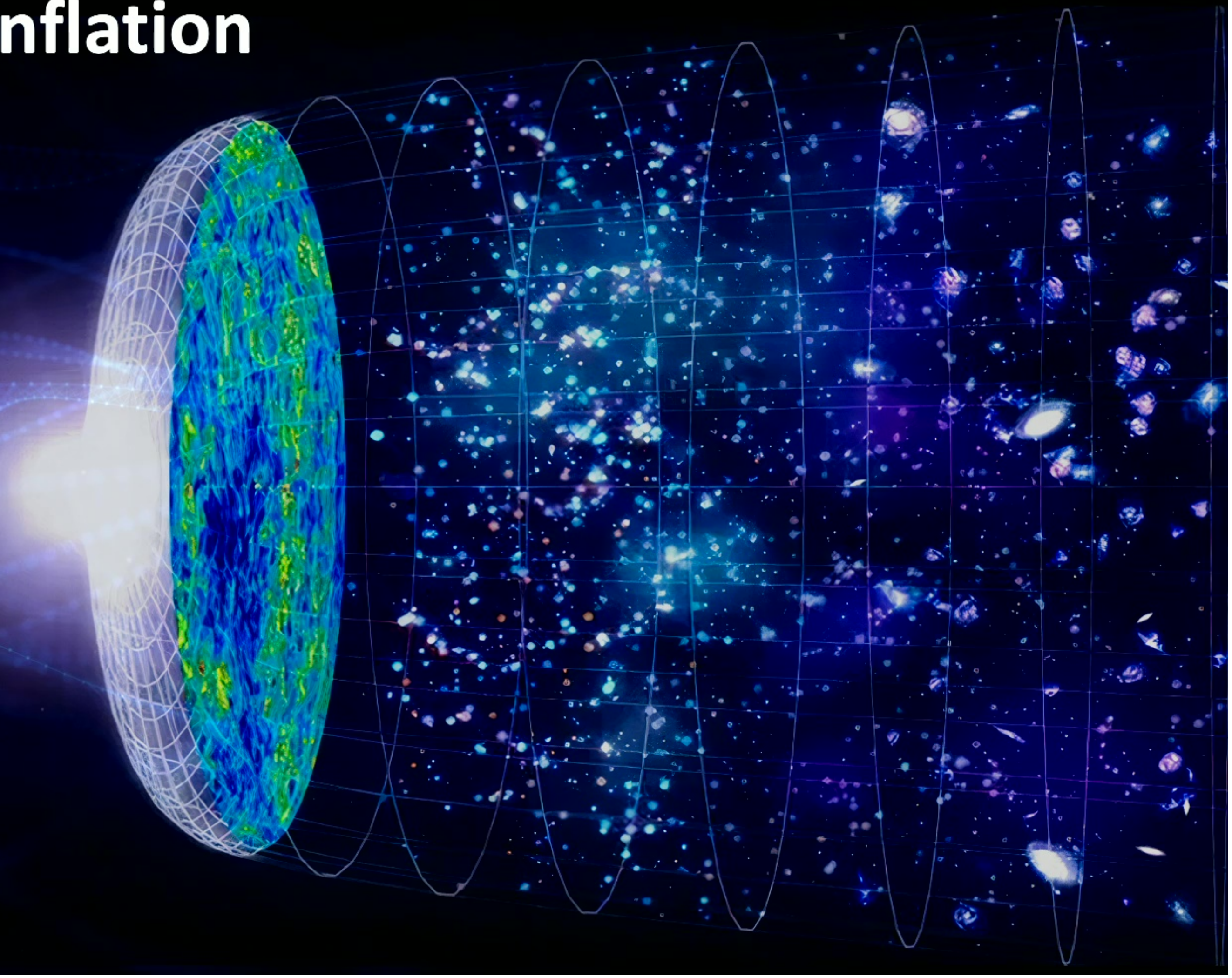

Inflation: a link between cosmic scales

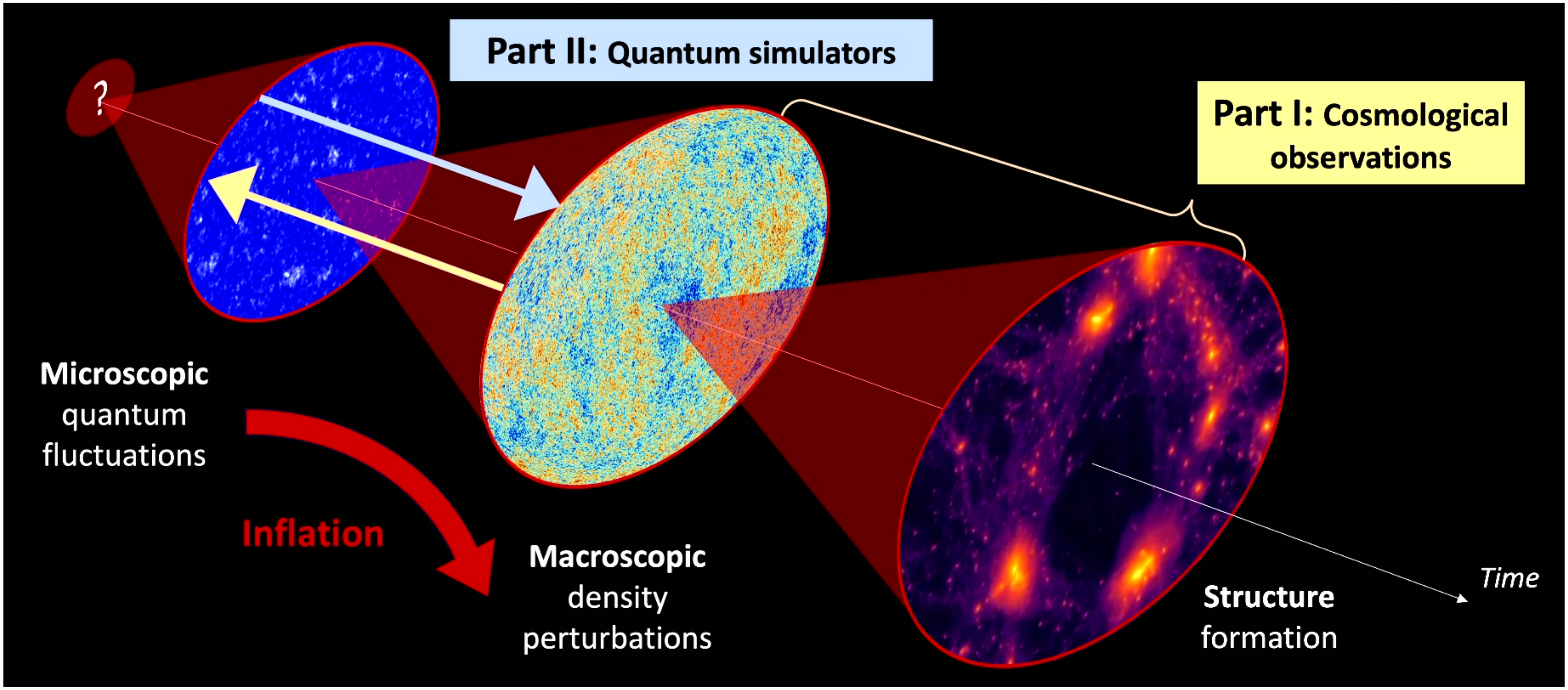
Part II: **Quantum simulators**

Part I: **Cosmological observations**

Part I – CMB constraints

Inflationary prediction: nearly scale-invariant spectrum of primordial **density fluctuations**

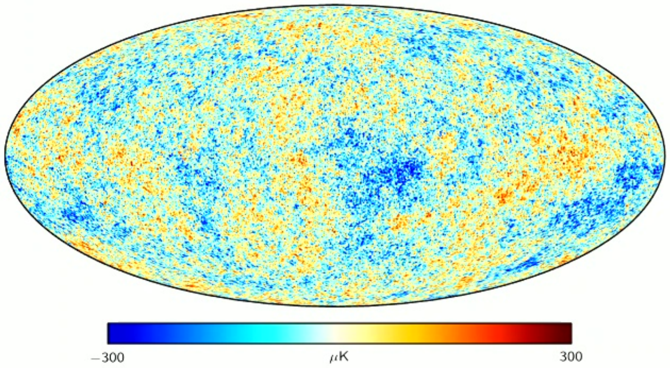

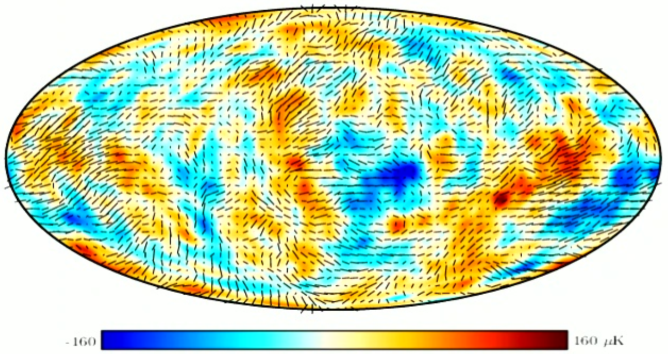

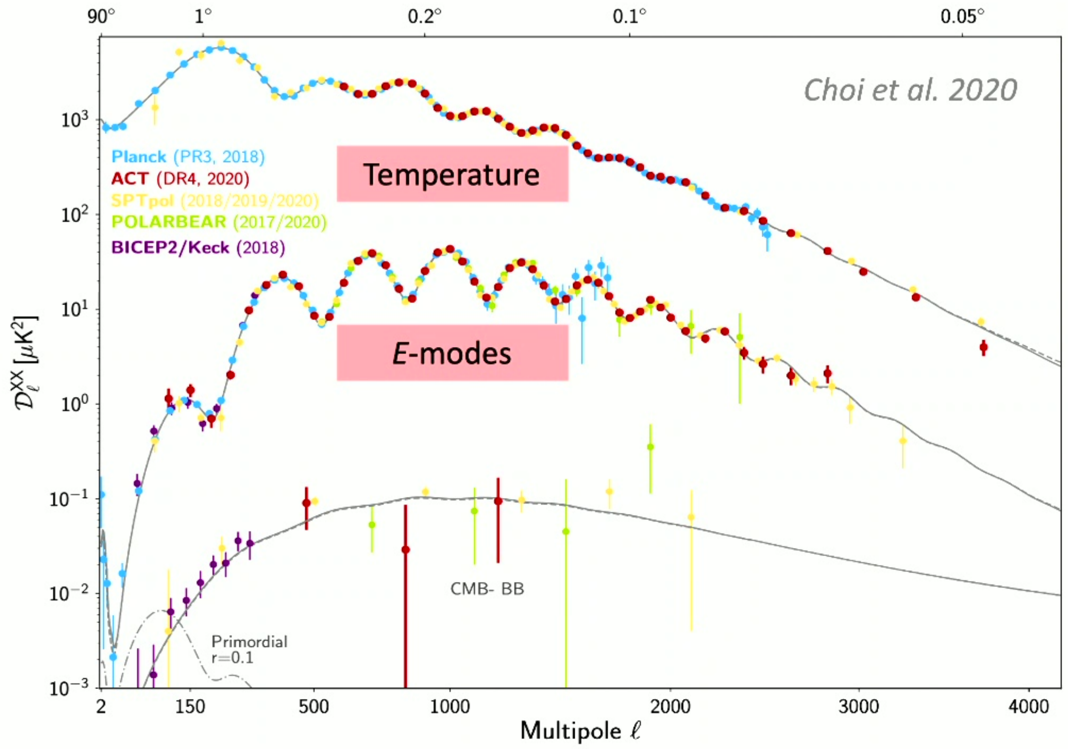

From inflation to CMB polarization

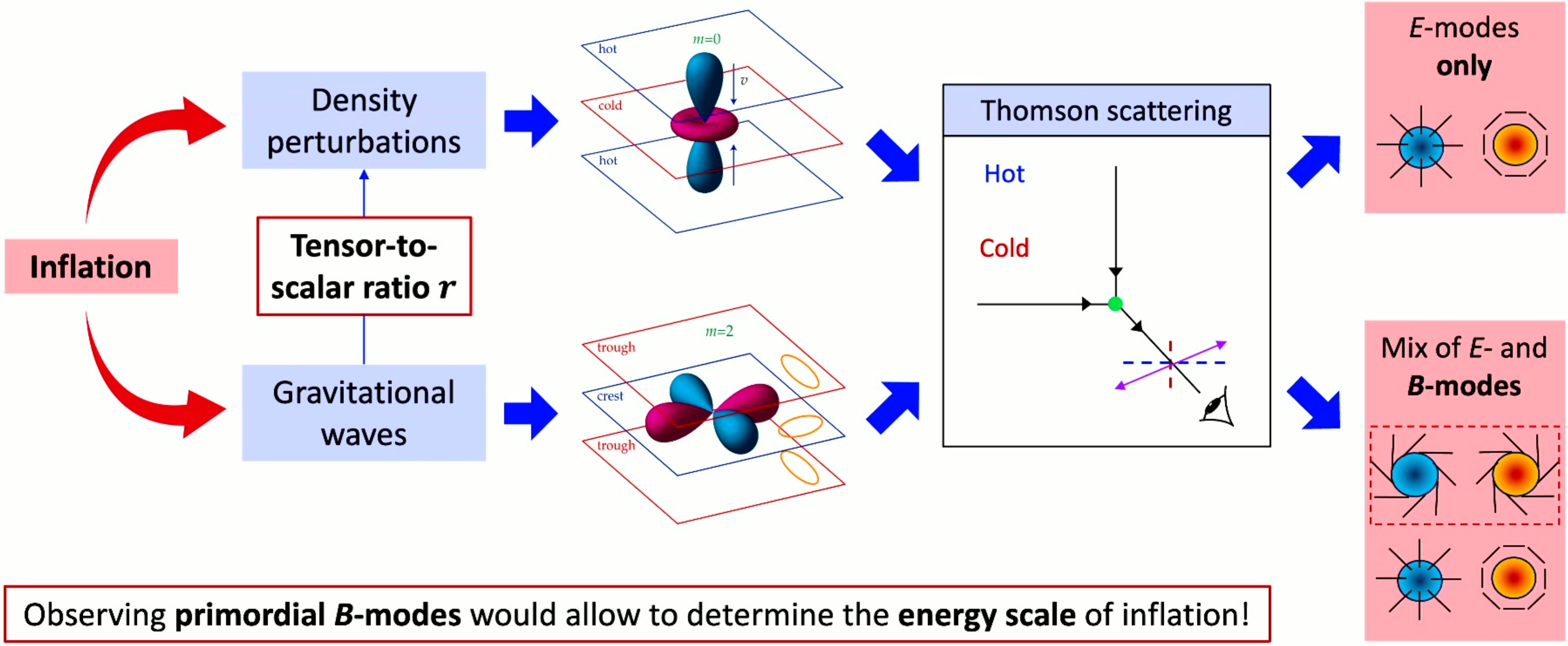

Inflation

Density perturbations

Tensor-to-scalar ratio r

Gravitational waves

Thomson scattering

Hot

Cold

E-modes **only**

Mix of *E*- and ***B*-modes**

Observing **primordial *B*-modes** would allow to determine the **energy scale** of inflation!

Recent constraints on primordial GW

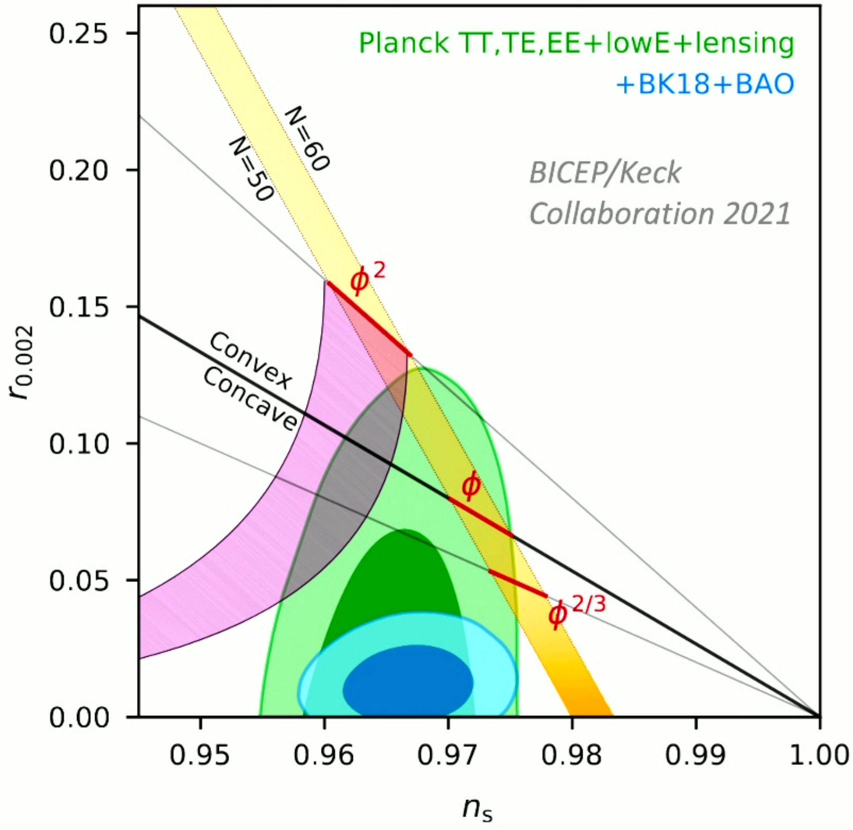

Current upper bound (95% confidence):

$$r < 0.036$$

Corresponding statistical uncertainty:

$$\sigma(r) = 0.009$$

- Some of the **simplest** inflation models now **excluded**, e.g. natural inflation (purple) and monomial potentials (orange)

Challenge 1: Galactic foregrounds

- **Dust** thermal emission
- **Synchrotron** radiation from cosmic ray electrons

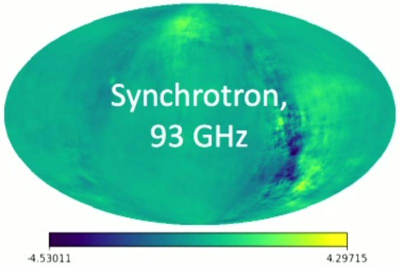

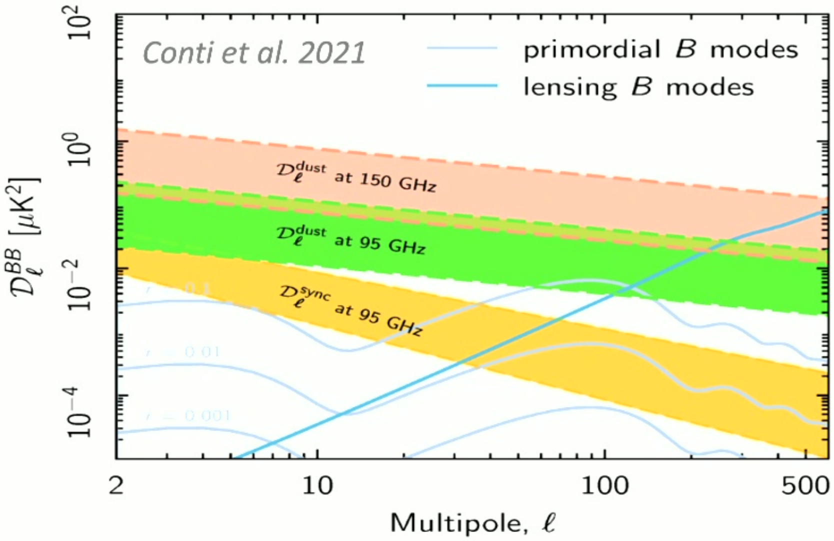

Rescaled spectral energy distributions (SEDs)

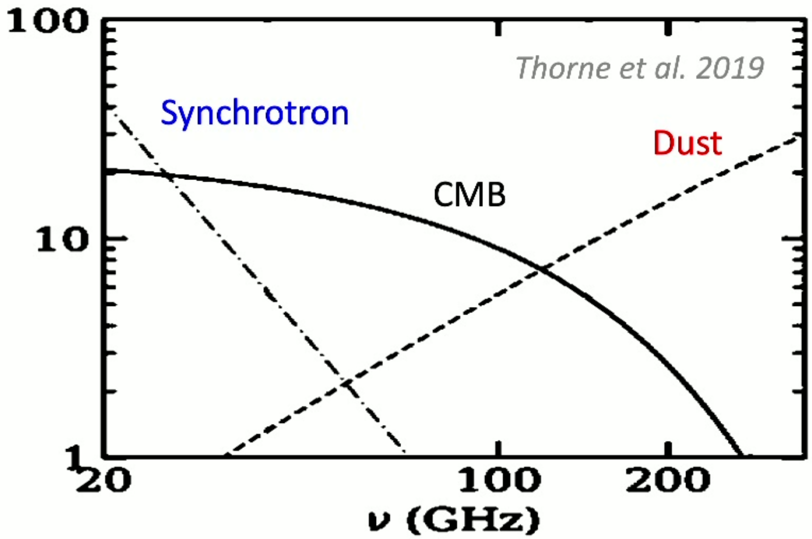

Foregrounds can be **distinguished** from the CMB by **multifrequency** observations

The Simons Observatory (SO): SATs

Small Aperture Telescopes

- Targeting faint, **large-scale *B*-modes** over approx. **10%** of the sky
- **Operational!**

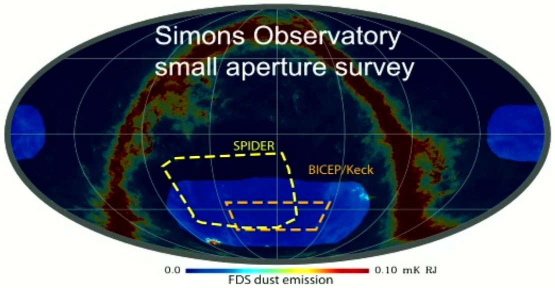

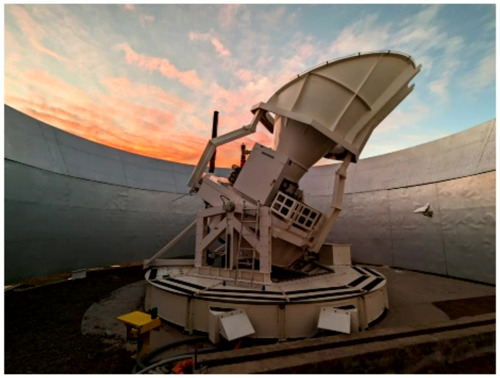

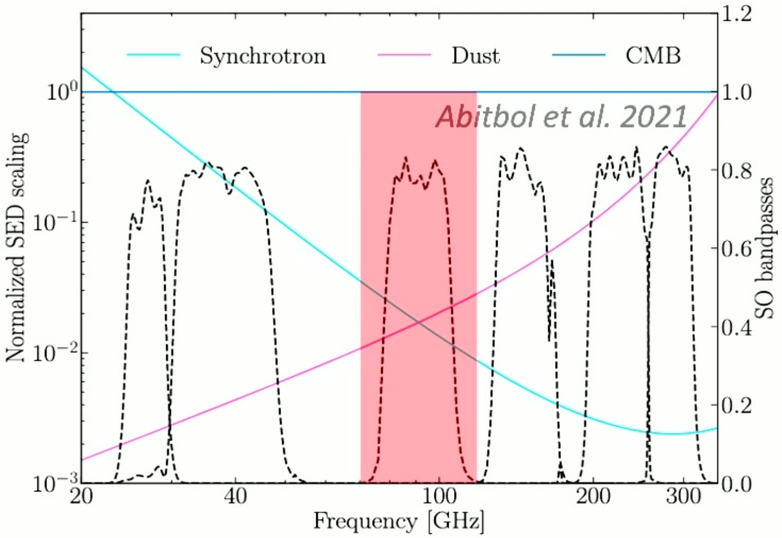

Abitbol et al. 2021

- **6 frequency bands** for component separation
- Most sensitive one at **93 GHz**, where foreground intensity is the lowest

Challenge 2: weak lensing

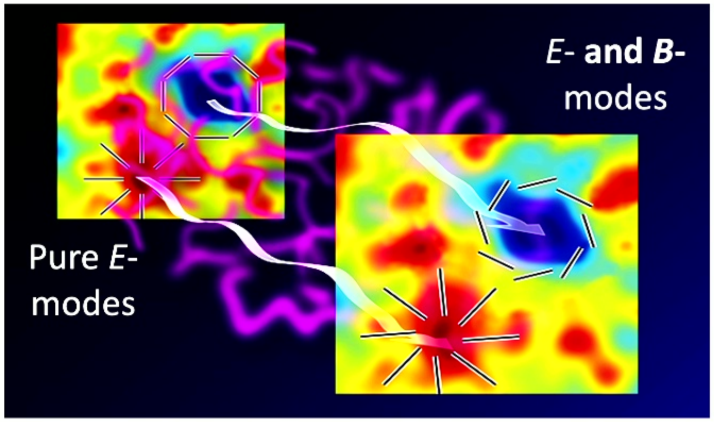

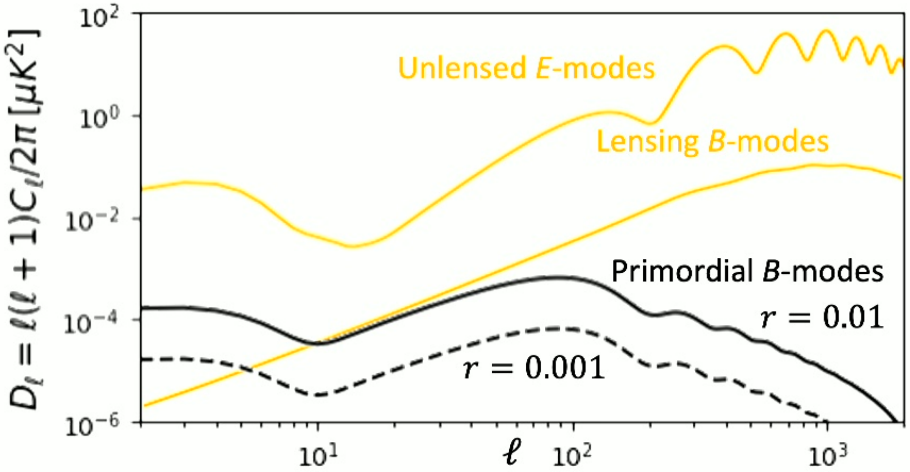

$$B_{\boldsymbol{l}}^{\text{lens}} = \sum_{\boldsymbol{l}'\boldsymbol{L}} f(\boldsymbol{l},\boldsymbol{l}',\boldsymbol{L})\, E^*_{\boldsymbol{l}'}\kappa^*_{\boldsymbol{L}}$$

We need to build a model **(template) of the lensing *B*-modes** from measurements of E and κ

Variance on *r* from Fisher information (Gaussian likelihood):

$$\sigma^{-2}(r)\Big|_{r=0} = \sum_{l} \frac{2l+1}{2}\left(\frac{\partial_r C_l}{C_l^{\text{lens}} + N_l}\right)^2$$

The Simons Observatory (SO): LAT

Large Aperture Telescope

- Still under construction, will **start operations in 2025**

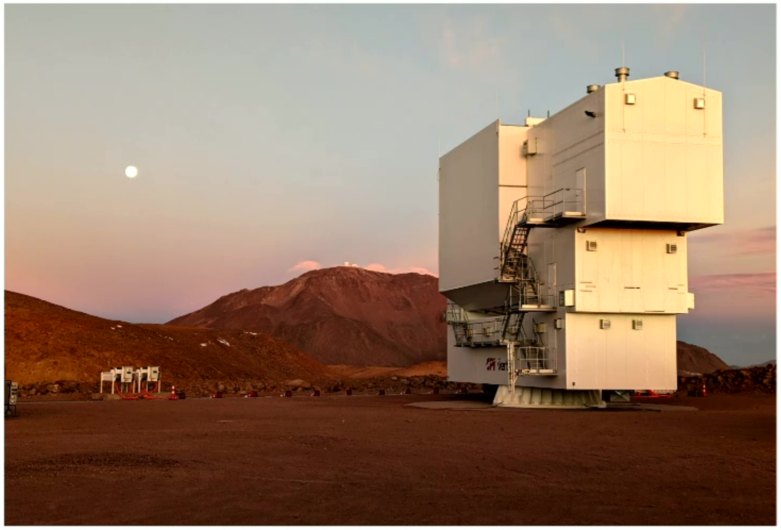

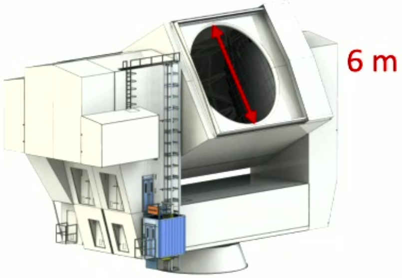

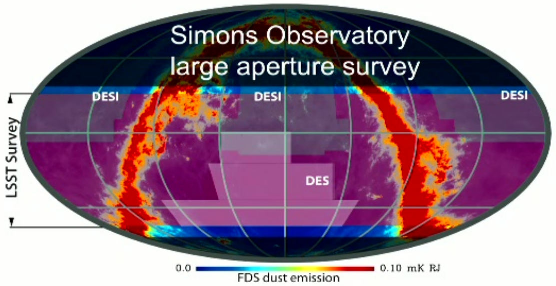

- Will provide **high-resolution** temperature and ***E*-mode** measurements needed for **lensing template**

- Will observe a larger area (approx. **40% of the sky**), **overlapping** with several galaxy surveys

Multitracer lensing reconstruction

- **Quadratic estimators** using data from the LAT
  - Off-diagonal correlations between pairs of lensed fields (***TT, TE, EE* and *EB***)
  - Accurate on large scales, noisy at high multipoles

- Complement with cosmic infrared background (**CIB**) and **galaxy survey data**

The **optimal convergence estimator** is a **weighted sum** of internal and external tracers

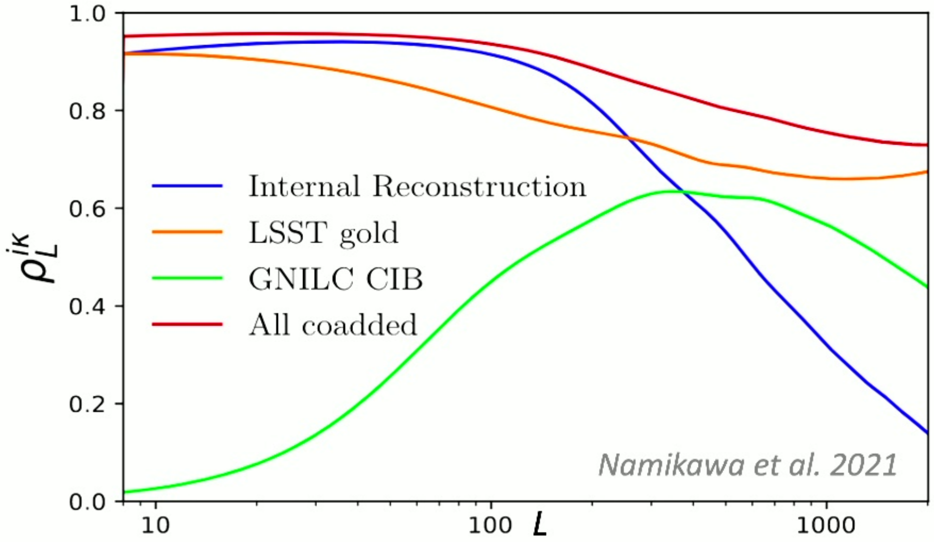

Namikawa et al. 2021

$$\hat{\kappa}^{\rm comb}_{LM} = \sum_i c_i\, \hat{\kappa}^i_{LM}$$

$$c_i = \sum_j (\boldsymbol{\rho}^{-1})_{ij}\,\rho_{j\kappa}\sqrt{C_l^{\kappa\kappa}/C_l^{ij}}$$

Maximizing $\rho^{\hat{\kappa}_{\rm comb}\kappa}$

Template construction pipeline

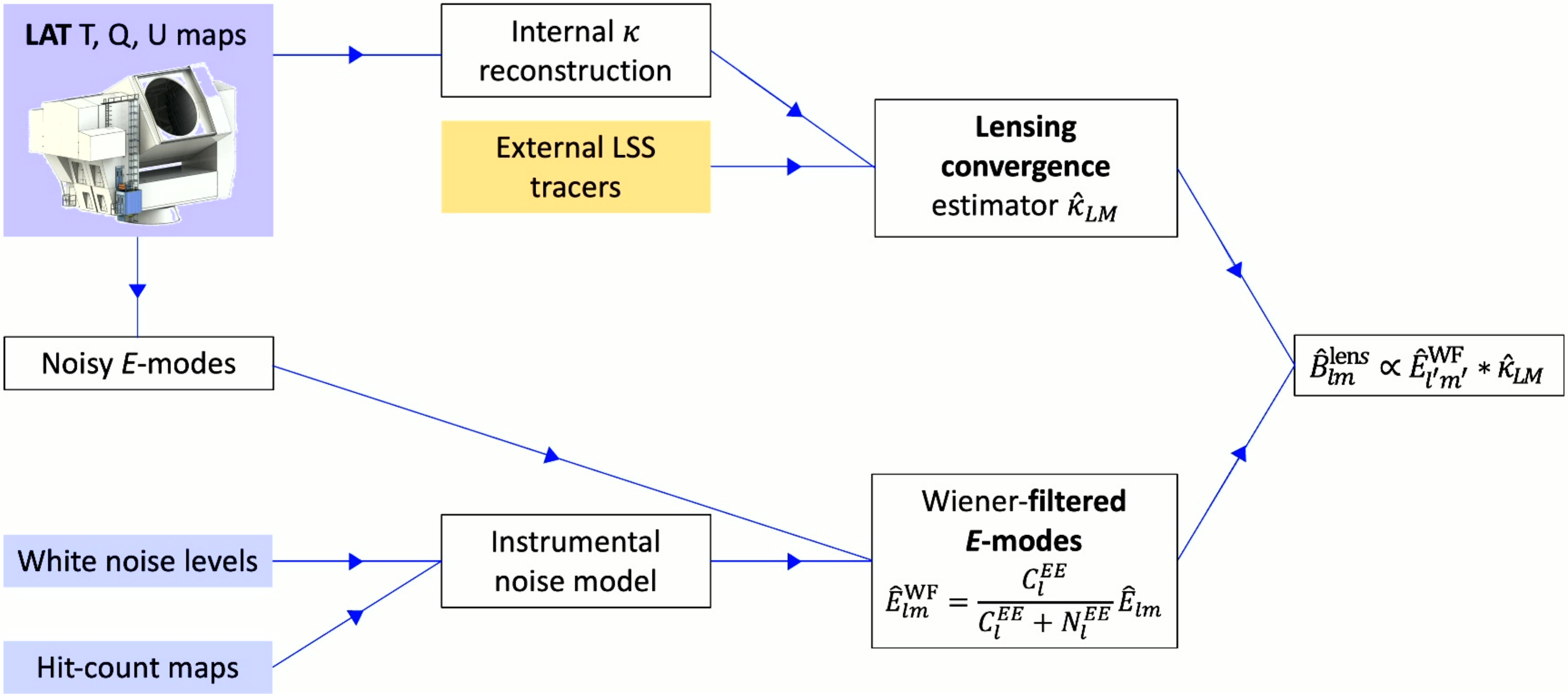

LAT T, Q, U maps

Internal κ reconstruction

External LSS tracers

Lensing convergence estimator $\hat{\kappa}_{LM}$

Noisy *E*-modes

White noise levels

Hit-count maps

Instrumental noise model

Wiener-**filtered** ***E*-modes**

$$\hat{E}^{\mathrm{WF}}_{lm} = \frac{C_l^{EE}}{C_l^{EE} + N_l^{EE}} \hat{E}_{lm}$$

$$\hat{B}^{\mathrm{lens}}_{lm} \propto \hat{E}^{\mathrm{WF}}_{l'm'} * \hat{\kappa}_{LM}$$

Forecasted delensing efficiency

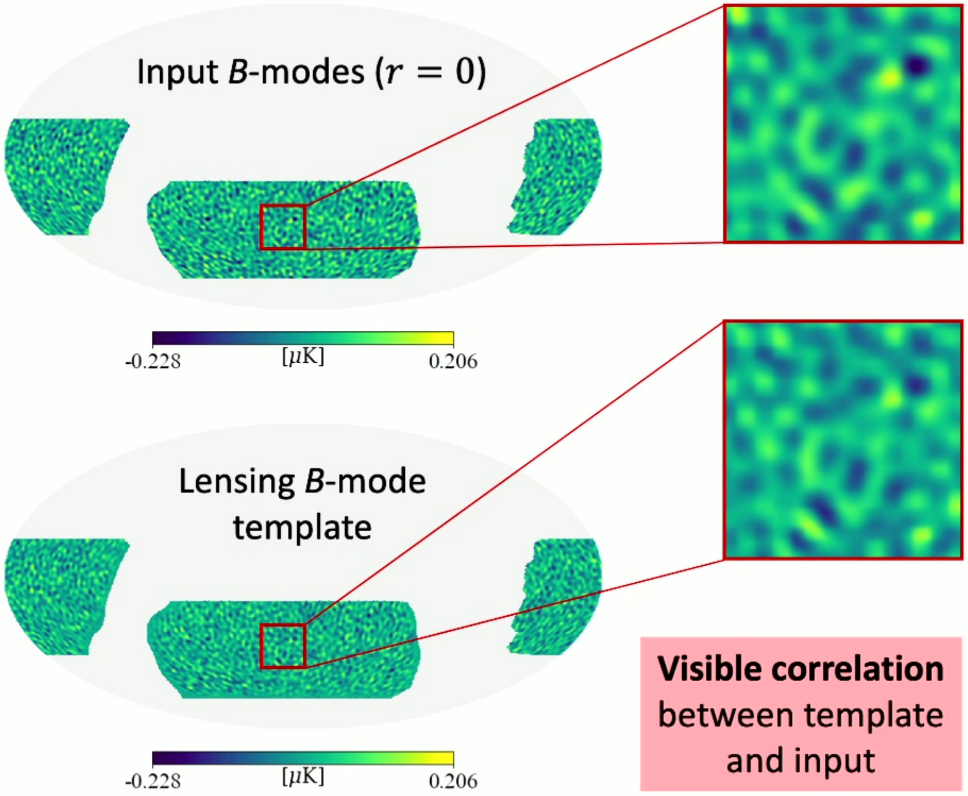

Visible correlation between template and input

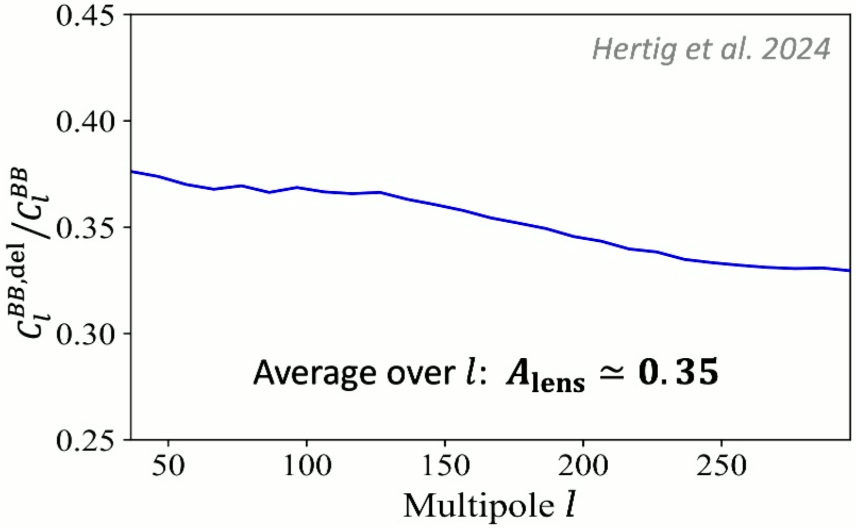

Hertig et al. 2024

Average over l: $A_{\mathrm{lens}} \simeq \mathbf{0.35}$

65% delensing efficiency achieved with LAT-like simulations at goal noise level

Component separation pipeline

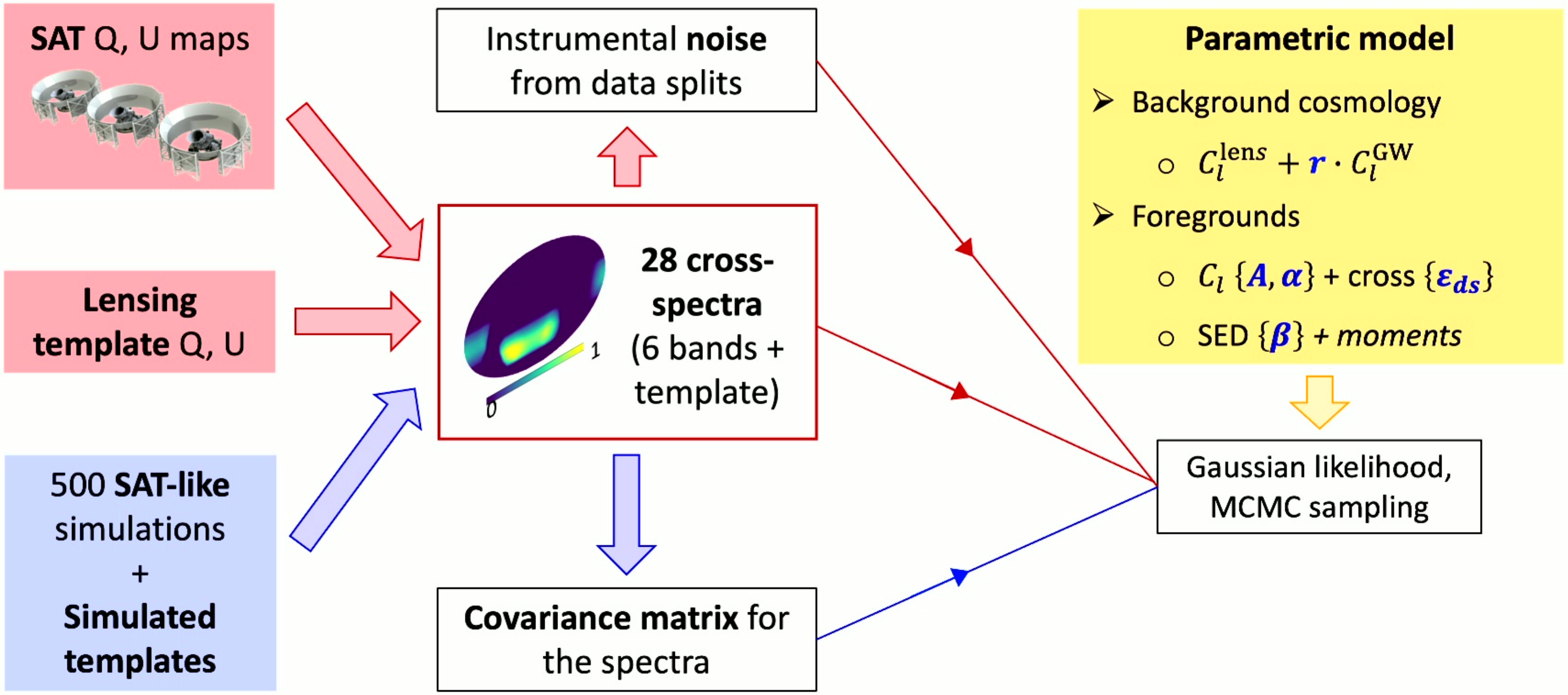

SAT Q, U maps

Lensing template Q, U

500 **SAT-like** simulations + **Simulated templates**

Instrumental **noise** from data splits

28 cross-spectra (6 bands + template)

Covariance matrix for the spectra

Parametric model

- Background cosmology
  - $C_l^{\text{lens}} + r \cdot C_l^{\text{GW}}$
- Foregrounds
  - $C_l\ \{A, \alpha\}$ + cross $\{\varepsilon_{ds}\}$
  - SED $\{\beta\}$ + *moments*

Gaussian likelihood, MCMC sampling

Foreground model

- Power spectra modelled as **power laws** $C_l^{d/s} = \boldsymbol{A_{d/s}} \left(\frac{l}{l_0}\right)^{\boldsymbol{\alpha_{d/s}}-2}$

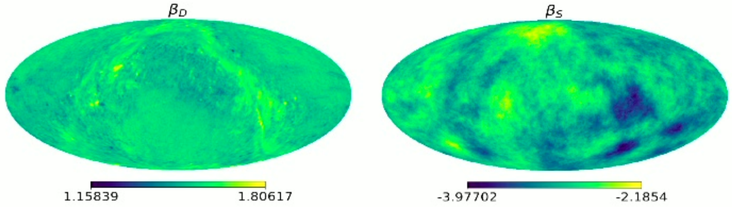

- Spectral energy distributions (**SEDs**):
  - Dust: $\bar{S}_\nu^d \propto \nu^{\boldsymbol{\beta_d}} B_\nu(T_d)$
  - Synchrotron: $\bar{S}_\nu^s \propto \nu^{\boldsymbol{\beta_s}}$

Foreground **SEDs vary in space** due to inhomogeneous **dust temperature / grain types** and fluctuations in the **cosmic ray energy distribution.**

- Leading order term (**sky average**):

$$C_{l,0}^{\nu\nu'} = \bar{S}_\nu^d \bar{S}_{\nu'}^d C_l^d + \bar{S}_\nu^s \bar{S}_{\nu'}^s C_l^s$$

$$+ \left(\bar{S}_\nu^d \bar{S}_{\nu'}^s + \bar{S}_\nu^s \bar{S}_{\nu'}^d\right) \boldsymbol{\epsilon_{ds}} \sqrt{C_l^d C_l^s}$$

Second order expansion of SEDs:

$$S_\nu\big(\beta(\hat{n})\big) = S_\nu\big(\bar{\beta}\big) + \partial_\beta S_\nu \cdot \delta\beta(\hat{n}) + \frac{1}{2}\partial_\beta^2 S_\nu \cdot \big(\delta\beta(\hat{n})\big)^2$$

« **Moment expansion** » of foreground power spectra:

extra terms containing $C_l^{\beta\beta} = \boldsymbol{B_{d/s}}(l/l_0)^{\boldsymbol{\gamma_{d/s}}}$

Chluba et al. 2017

Parameter inference example

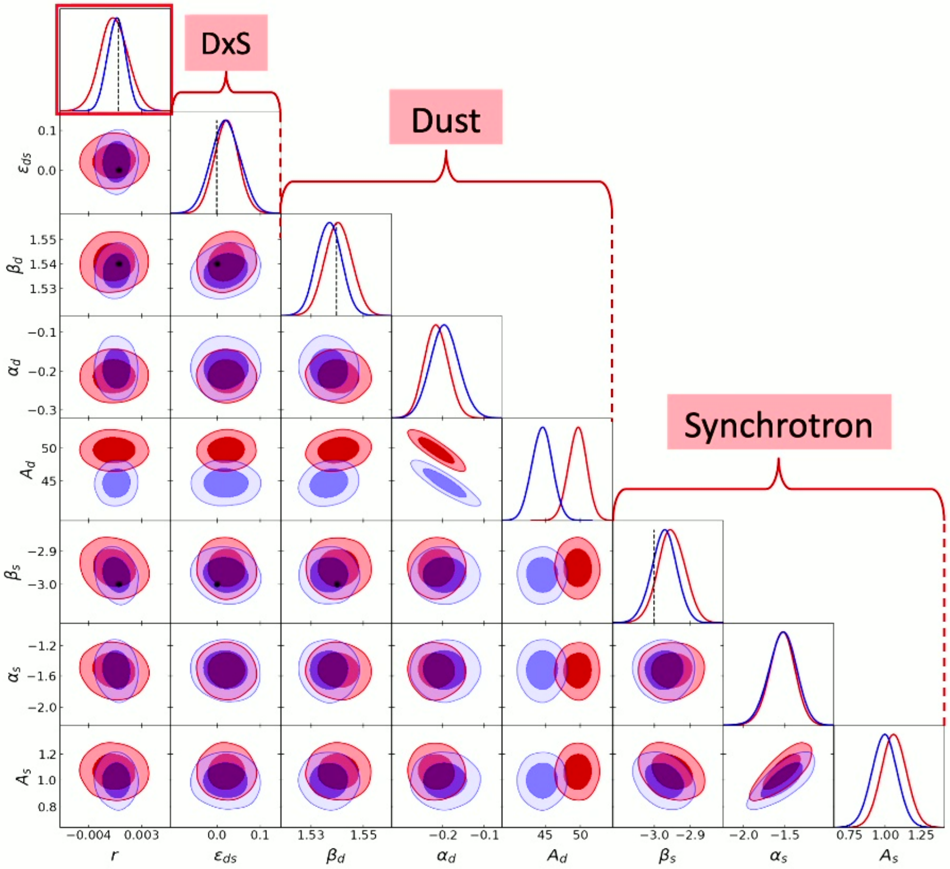

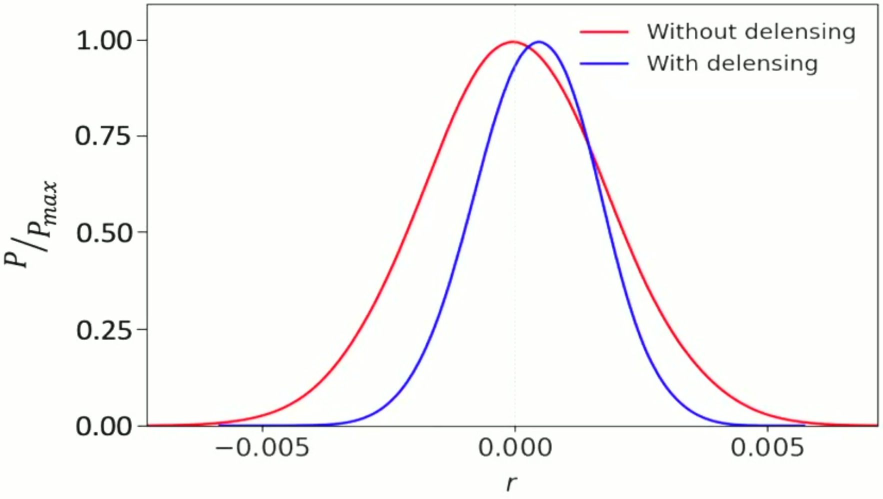

	$\sigma(r)$
Without delensing	$1.9 \cdot 10^{-3}$
With delensing	$1.2 \cdot 10^{-3}$
$A_{\text{lens}} = 0.35$ input	$1.2 \cdot 10^{-3}$

Performance forecasts for SO Nominal

Mean of best-fit r and MCMC standard deviations for 100 realizations

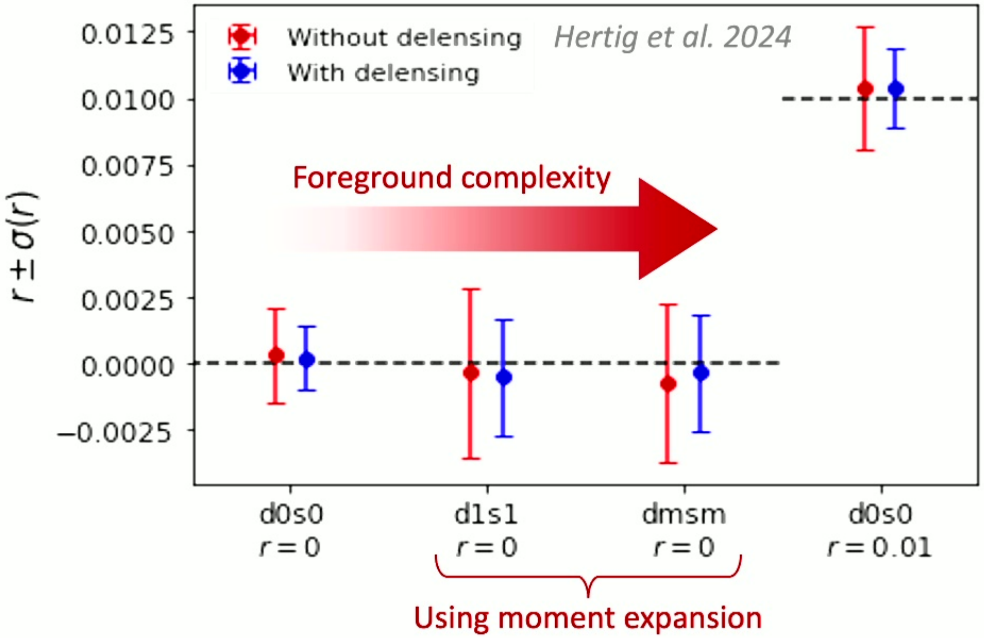

Main takeaways

- **No significant bias** within statistical uncertainties
- Error bars are reduced by ~**30% to 40%** depending on foreground complexity
- **Nonzero r** successfully detected

SO's target precision $\sigma(r)|_{r=0} = 0.003$ is achieved for all models after delensing

Towards application to real data

Goal: build a **lensing template from external tracers** for early SO analysis

ACT DR6 lensing reconstruction

$$W^{\kappa}(z) = \frac{3}{2H(z)}\Omega_m H_0^2(1+z)\chi(z)\left(\frac{\chi_* - \chi(z)}{\chi_*}\right)$$

- Minimum-variance combination of TT, TE, EE and EB **quadratic estimators**

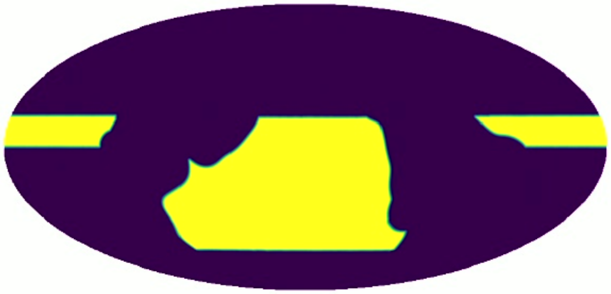

unWISE **blue** and **green** galaxy samples

$$W^{g}(z) = \frac{b(z)\ dN/dz}{\int dz'(dN/dz')}$$

- Fit **linear bias** model to $C_l^{\kappa g}$

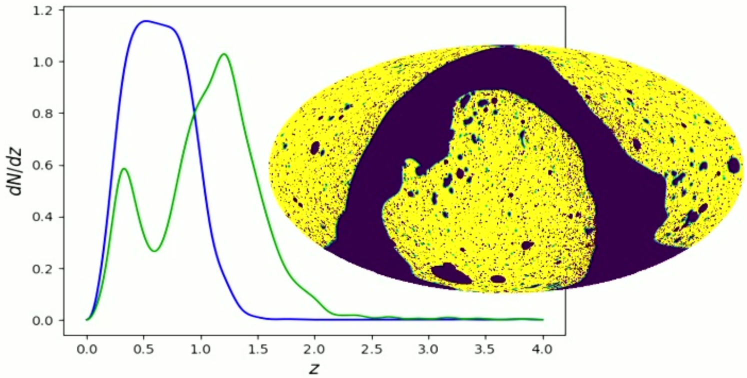

Towards application to real data

Goal: build a **lensing template from external tracers** for early SO analysis

Planck GNILC CIB

$$W^I(z) = \boldsymbol{b_c} \frac{\chi^2(z)}{H(z)(1+z)^2} e^{-\frac{(z-z_c)^2}{2\sigma_z^2}} f_{\nu(1+z)}$$

- Fit **amplitude** $\boldsymbol{b_c}$ to $C_l^{\kappa I}$

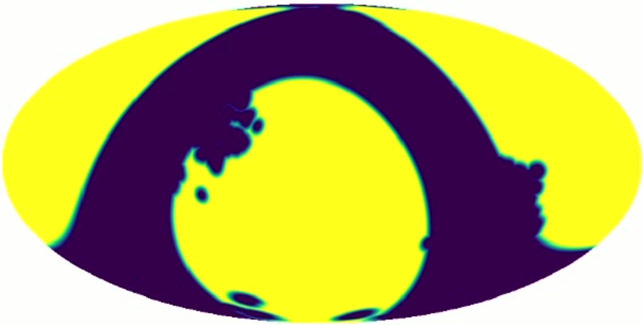

$$C_l^{\kappa i} = \int_0^{z_*} \frac{dzH(z)}{\chi^2(z)} W^\kappa(z) W^i(z) P_k(z)$$

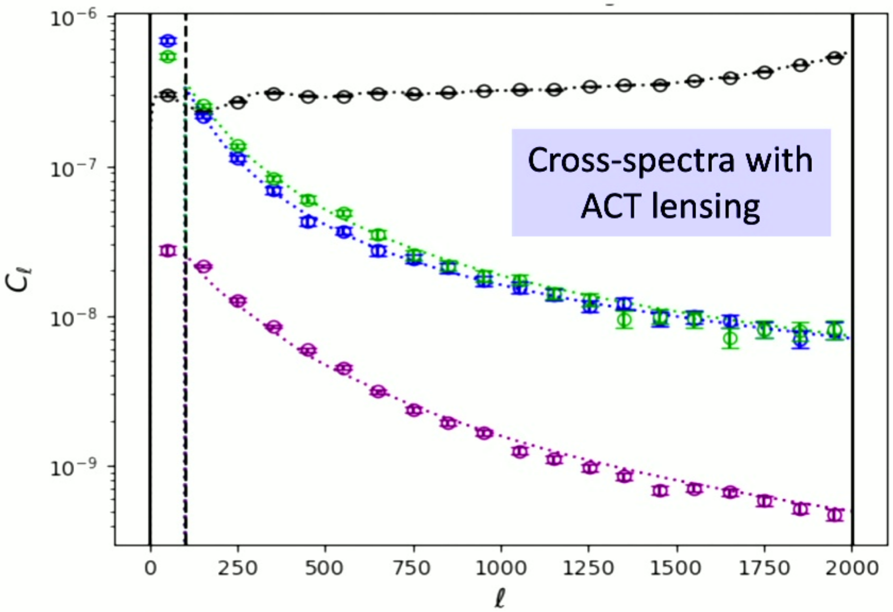

Cross-spectra with ACT lensing

Combined lensing estimator

Cross-spectra between external tracers

- Include shot noise and dust contamination
- Too simplistic for C_l between galaxy samples

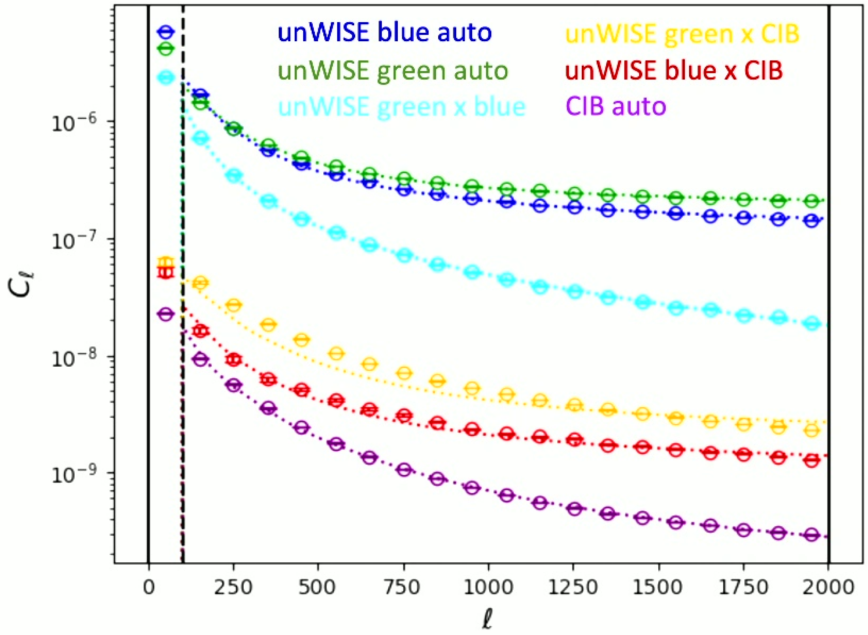

Correlation coefficients with true κ

- For combined tracer, estimated using

$$\rho_L^{\kappa\hat{\kappa}_{\text{comb}}} = \rho_L^{\hat{\kappa}_{\text{comb}}\hat{\kappa}_{\text{comb}}}$$

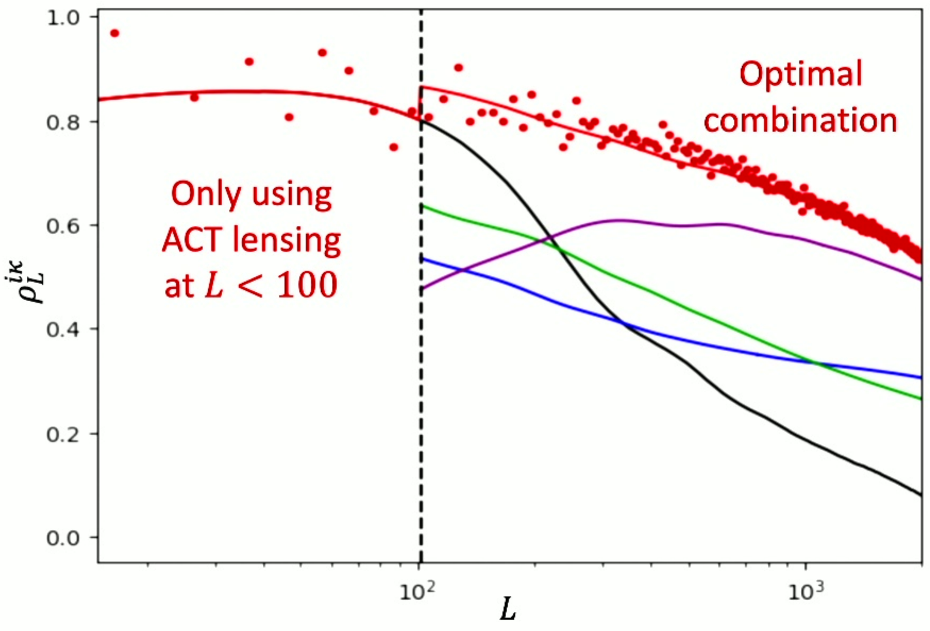

Only using ACT lensing at $L < 100$

Optimal combination

Template characterization

Template auto-spectrum and cross-spectrum with **Planck SMICA *B*-modes**

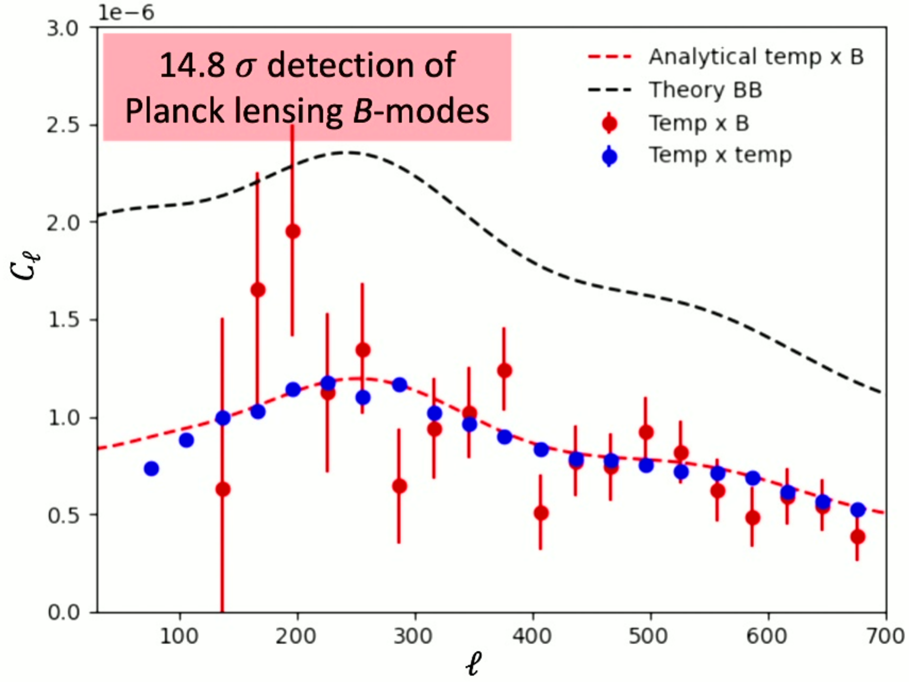
14.8 σ detection of Planck lensing *B*-modes

Delensing efficiency: fractional decrease in lensing *B*-mode power

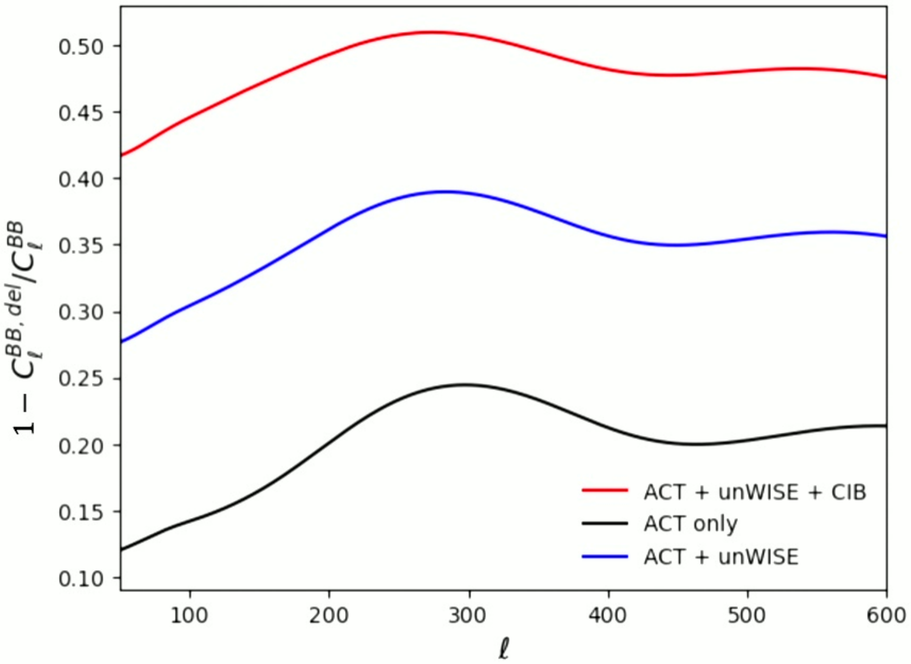

Future prospects

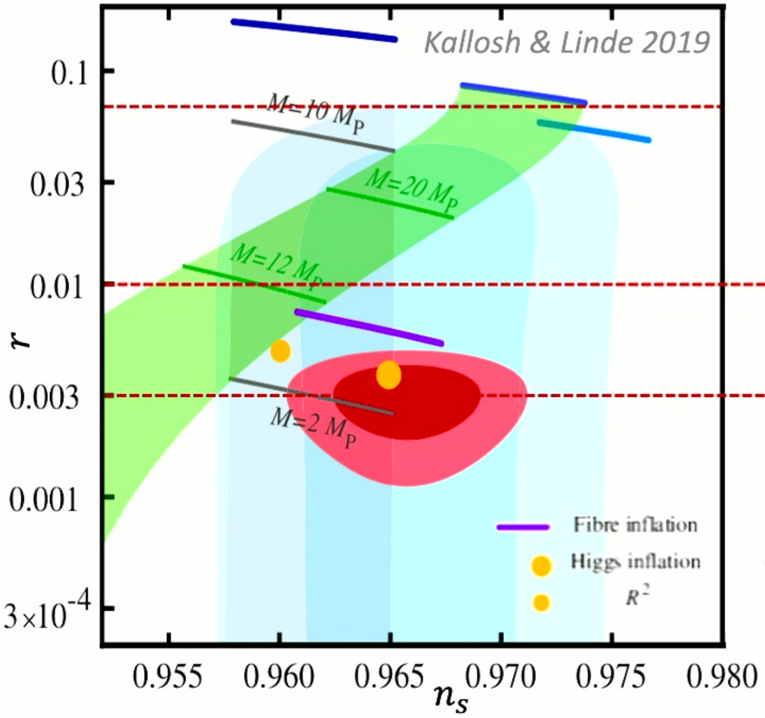

Current upper bound on r

Delensing will become **increasingly important** as noise levels continue diminishing!

Our forecasts

$r < 0.01$

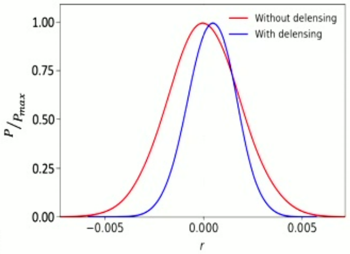

Additional SO SATs (**2026**)

LiteBIRD, CMB-S4, ...

$r < 0.003$

2030s

Part II – Simulating false vacuum decay

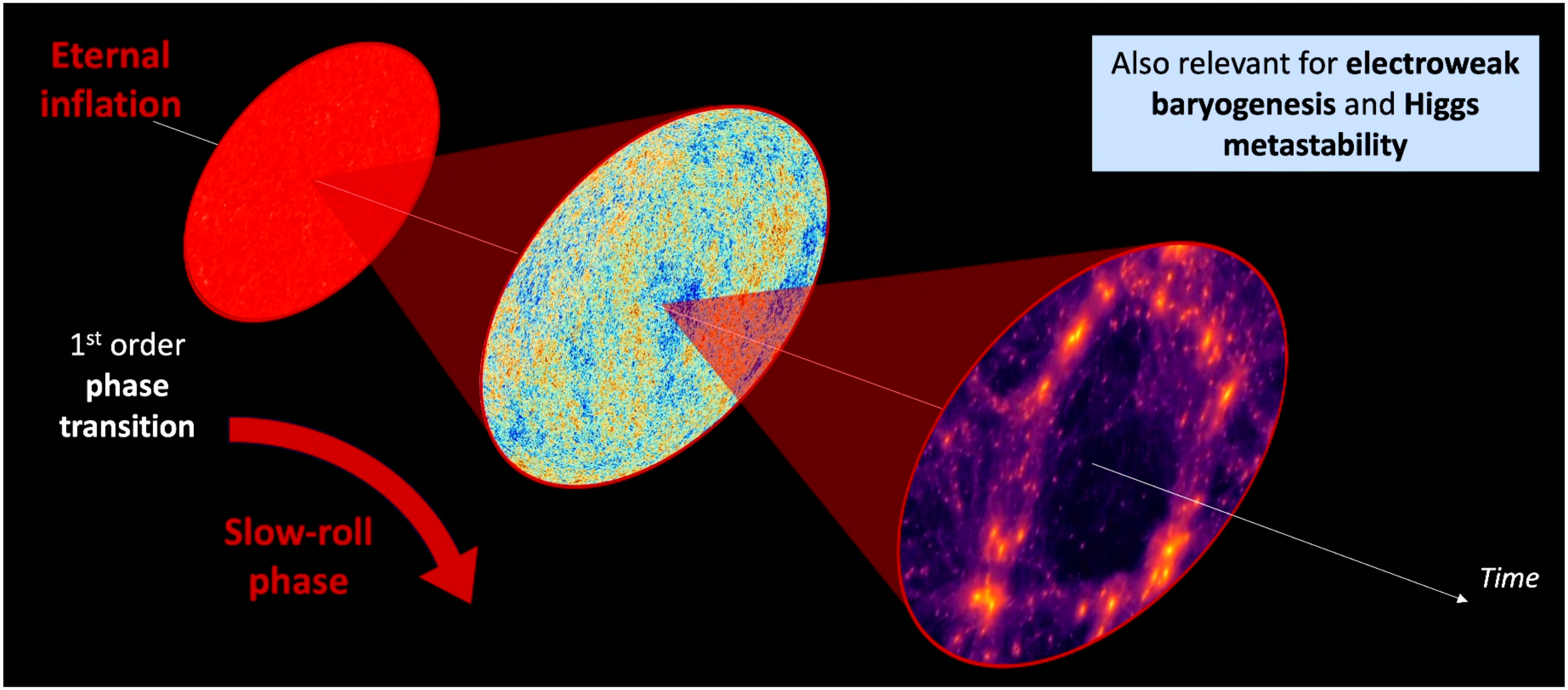

Also relevant for **electroweak baryogenesis** and **Higgs metastability**

Instanton formalism

Relativistic scalar field in D + 1 dimensions: $\mathcal{L} = \frac{1}{2}\partial_\mu\phi\partial^\mu\phi - V(\phi)$

- Path integral in **Euclidean time** $\tau = it$

$$\langle\phi_{TV}|e^{-\frac{\hat{H}\tau}{\hbar}}|\phi_{FV}\rangle = \int \mathcal{D}[\phi]e^{-\frac{S_E}{\hbar}}$$

$$S_E = \int d\tau d^D\vec{x}\left[\frac{1}{2}\left(\frac{\partial\phi}{\partial\tau}\right)^2 + \frac{1}{2}\left(\vec{\nabla}\phi\right)^2 + V(\phi)\right]$$

Minimizing S_E:

$$(\partial_\tau^2 + \nabla^2)\phi = V'(\phi)$$

- Assuming $\boldsymbol{O(D+1)}$ **symmetry**

$$\frac{d^2\phi}{d\rho^2} + \frac{D}{\rho}\frac{d\phi}{d\rho} = V'(\phi) \quad \begin{cases} \rho = \sqrt{\tau^2 + |\vec{x}|^2} \\ d\phi/d\rho\big|_{\rho=0} = 0 \\ \phi(\rho=\infty) = \phi_{FV} \end{cases}$$

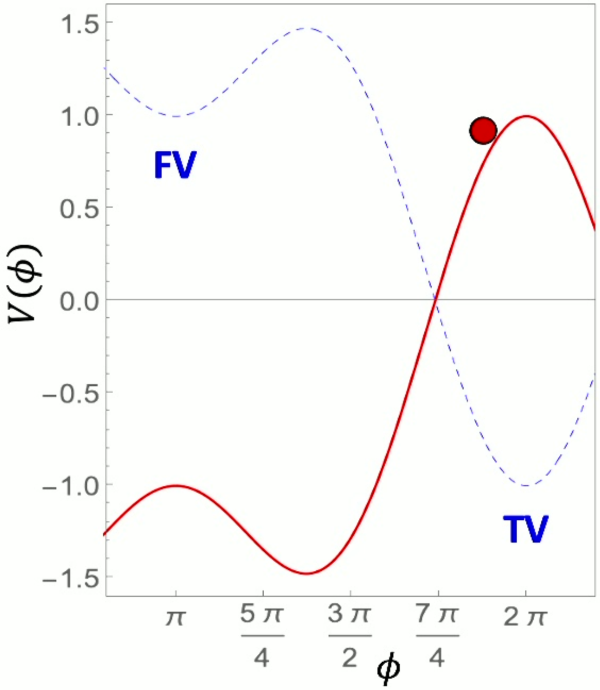

Classical particle path in **inverted potential**

Instanton formalism

Relativistic scalar field in D + 1 dimensions: $\mathcal{L} = \frac{1}{2}\partial_\mu\phi\partial^\mu\phi - V(\phi)$

- Path integral in **Euclidean time** $\tau = it$

$$\left.\begin{aligned} &\langle \phi_{TV}| e^{-\frac{\hat{H}\tau}{\hbar}} |\phi_{FV}\rangle = \int \mathcal{D}[\phi]\, e^{-\frac{S_E}{\hbar}} \\ &S_E = \int d\tau d^D\vec{x}\left[\frac{1}{2}\left(\frac{\partial\phi}{\partial\tau}\right)^2 + \frac{1}{2}\left(\vec{\nabla}\phi\right)^2 + V(\phi)\right] \end{aligned}\right\}$$

Minimizing S_E:

$$(\partial_\tau^2 + \nabla^2)\phi = V'(\phi)$$

- Assuming $\boldsymbol{O(D+1)}$ **symmetry**

$$\frac{d^2\phi}{d\rho^2} + \frac{D}{\rho}\frac{d\phi}{d\rho} = V'(\phi) \quad \left\{\begin{aligned} &\rho = \sqrt{\tau^2 + |\vec{x}|^2} \\ &d\phi/d\rho\big|_{\rho=0} = 0 \\ &\phi(\rho = \infty) = \phi_{FV} \end{aligned}\right.$$

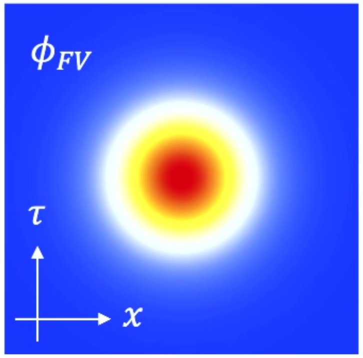

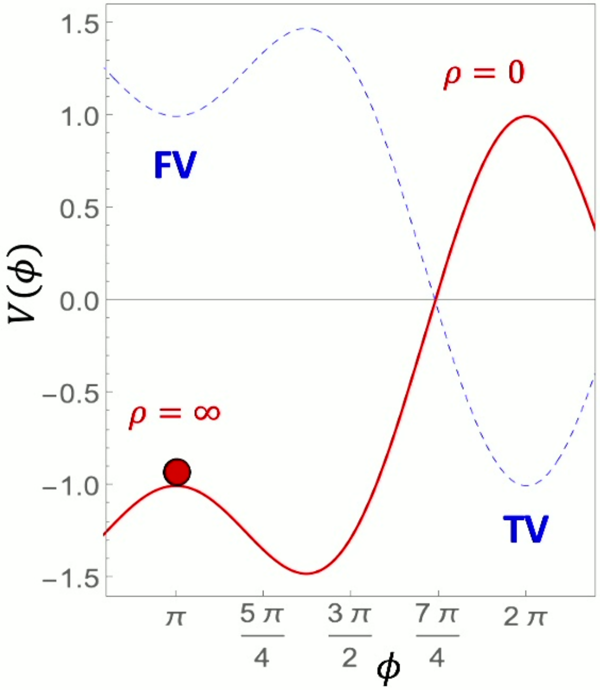

Classical particle path in **inverted potential**

Analytic continuation

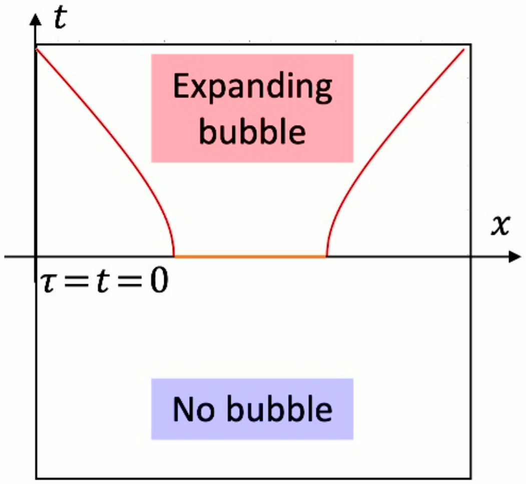

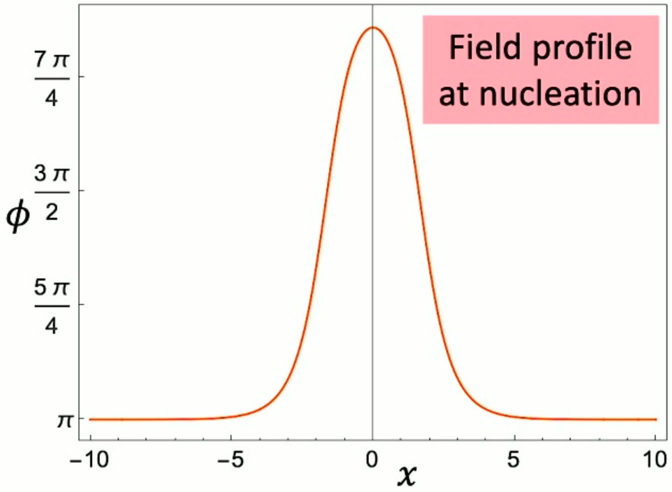

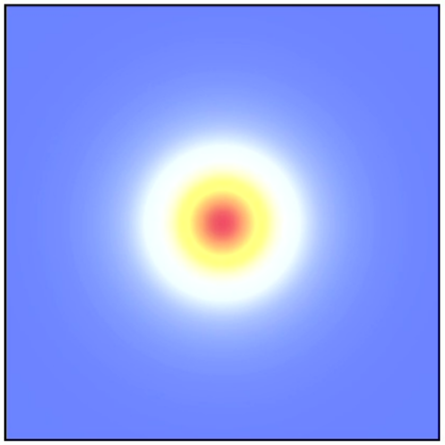

$t > 0$: classical evolution

Bubble wall at $\rho = R$

$\Longrightarrow$ hyperbolic trajectory

$$-t^2 + |\vec{x}|^2 = R^2$$

Thermal case

- Independent of τ at $T \gg 0$

$$\frac{d^2\phi}{dx^2} = V'(\phi)$$

Analytic continuation

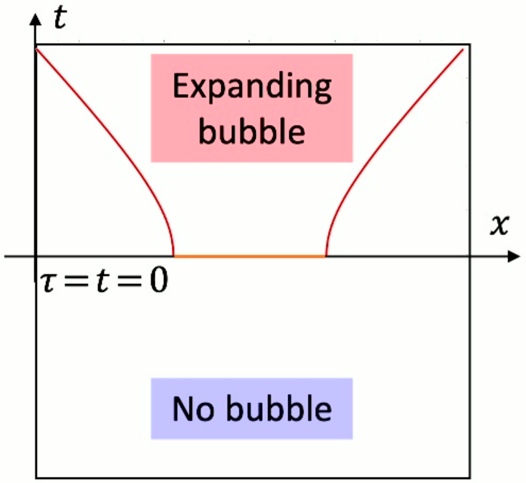

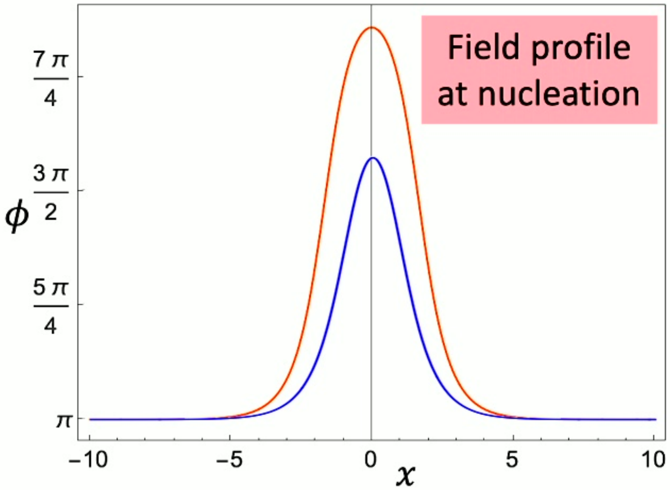

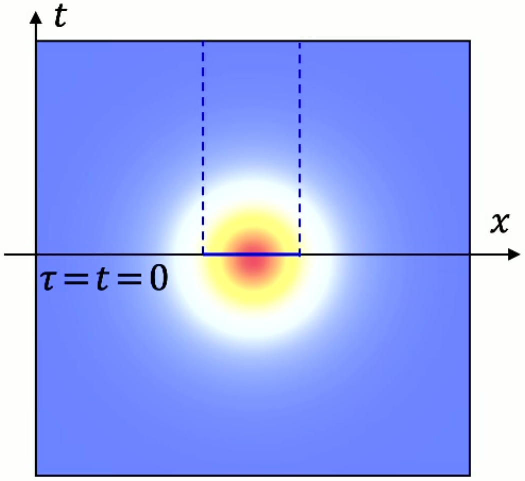

$t > 0$: classical evolution

Bubble wall at $\rho = R$

$\Longrightarrow$ hyperbolic trajectory

$$-t^2 + |\vec{x}|^2 = R^2$$

Thermal case

- Independent of τ at $T \gg 0$

$$\frac{d^2\phi}{dx^2} = V'(\phi)$$

- Fixed but **unstable** solution

Analytic continuation

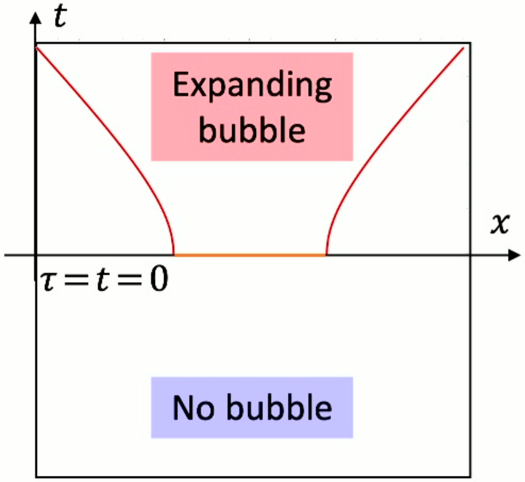

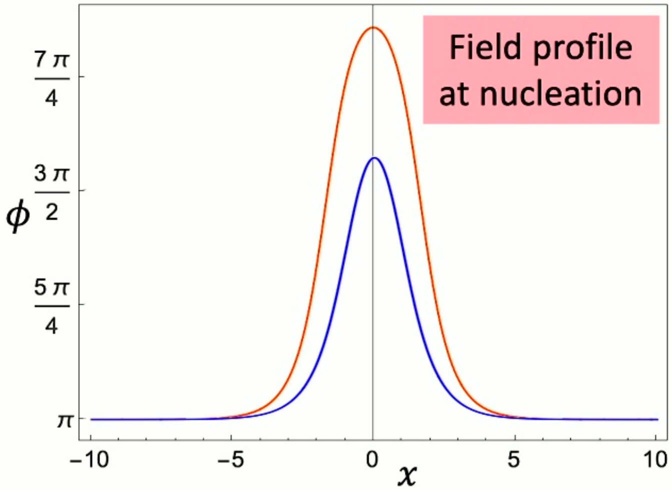

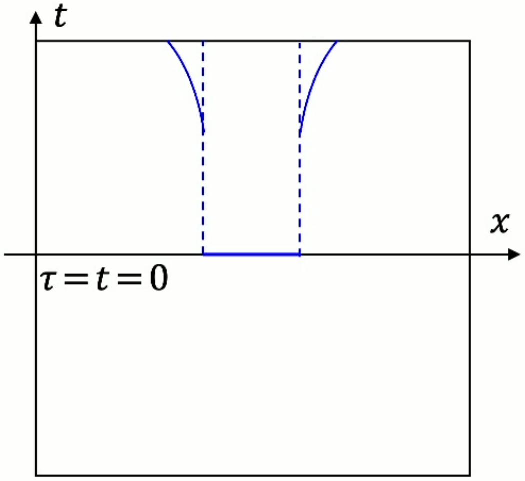

$t > 0$: classical evolution

Bubble wall at $\rho = R$

$\Longrightarrow$ hyperbolic trajectory

$$-t^2 + |\vec{x}|^2 = R^2$$

Missing information

⊗ Real-time nucleation dynamics

Thermal case

- Independent of τ at $T \gg 0$

$$\frac{d^2\phi}{dx^2} = V'(\phi)$$

- Fixed but **unstable** solution

Semiclassical lattice simulations

See Braden et al. 2019, arXiv:1806.06069

Step 1 – Quantum initial conditions

- Sample Gaussian fluctuations of free massive scalar field ($\hbar = c = 1$)

$$\langle \delta\phi_k^* \delta\phi_{k'} \rangle = \frac{1}{2\omega_k}\delta(k-k') \quad \langle \dot{\phi}_k^* \dot{\phi}_{k'} \rangle = \frac{\omega_k}{2}\delta(k-k')$$

with $\omega_k^2 = k^2 + m_{FV}^2 = k^2 + V''(\phi)|_{\phi_{FV}}$ and $\boldsymbol{k} \leq \boldsymbol{k_{UV}}$

Step 2 – Classical evolution

- Solve real-time Hamiltonian EoM with periodic BCs in space

$$\left.\begin{aligned} \Pi &= \dot{\phi} \\ \dot{\Pi} &= \nabla^2\phi - V'(\phi) \end{aligned}\right\}$$

✓ Real-time dynamics $\phi(x_i, t_i)$

Example in $1+1$D using A. Jenkins' *lattice-fvd* code

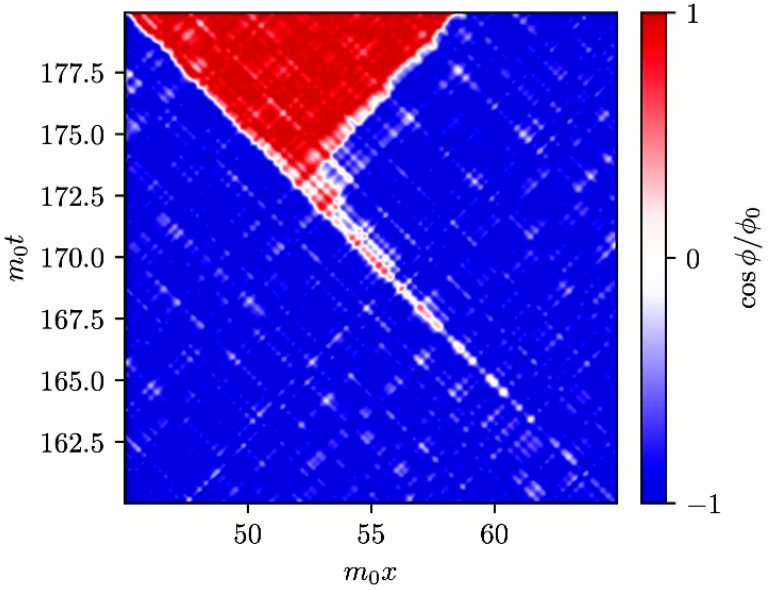

Semiclassical lattice simulations

See Braden et al. 2019, arXiv:1806.06069

Step 1 – Quantum initial conditions

- Sample Gaussian fluctuations of free massive scalar field ($\hbar = c = 1$)

$$\langle \delta\phi_k^* \delta\phi_{k'} \rangle = \frac{1}{2\omega_k}\delta(k-k') \qquad \langle \dot\phi_k^* \dot\phi_{k'} \rangle = \frac{\omega_k}{2}\delta(k-k')$$

with $\omega_k^2 = k^2 + m_{FV}^2 = k^2 + V''(\phi)|_{\phi_{FV}}$ and $\boldsymbol{k} \leq \boldsymbol{k_{UV}}$

Step 2 – Classical evolution

- Solve real-time Hamiltonian EoM with periodic BCs in space

$$\left.\begin{aligned} \Pi &= \dot\phi \\ \dot\Pi &= \nabla^2\phi - V'(\phi) \end{aligned}\right\}$$

✓ Real-time dynamics $\phi(x_i, t_i)$

✓ Truncated Wigner approximation

Example in $\mathbf{1+1D}$ using A. Jenkins' *lattice-fvd* code

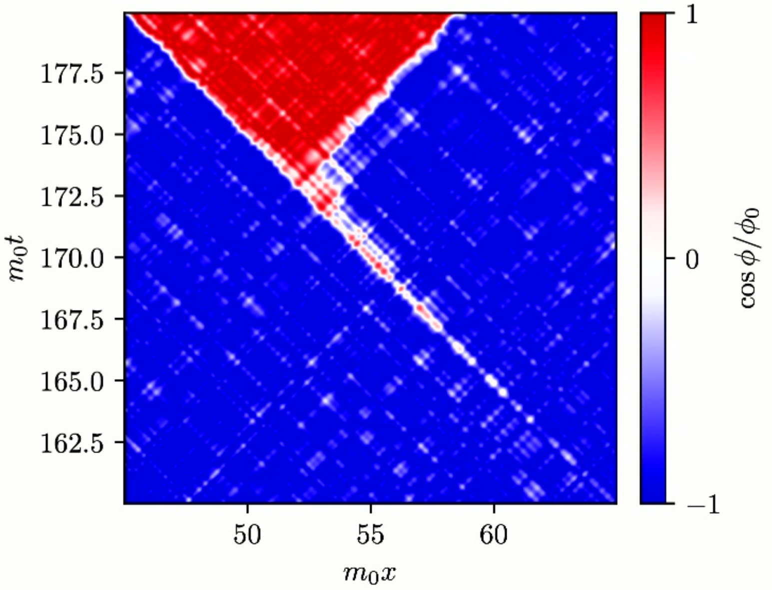

Decay rate comparison

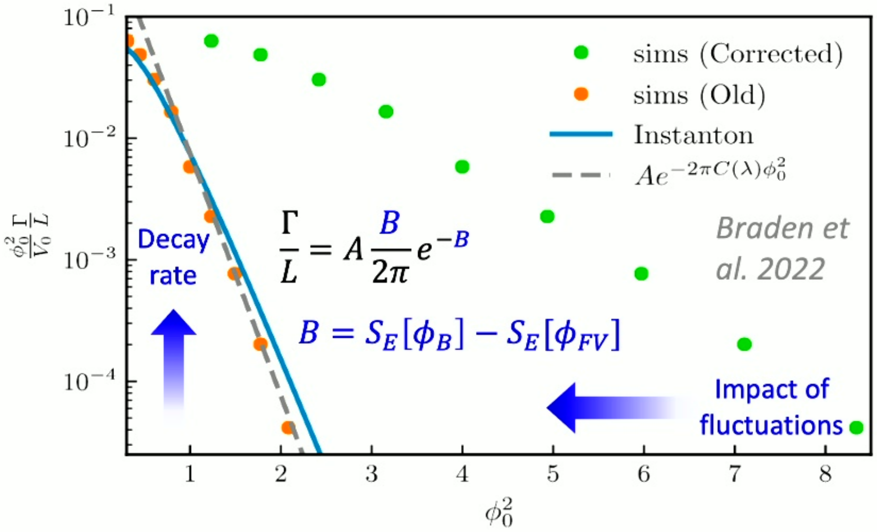

$$\frac{\Gamma}{L} = A\frac{B}{2\pi}e^{-B}$$

$$B = S_E[\phi_B] - S_E[\phi_{FV}]$$

Braden et al. 2022

Impact of fluctuations

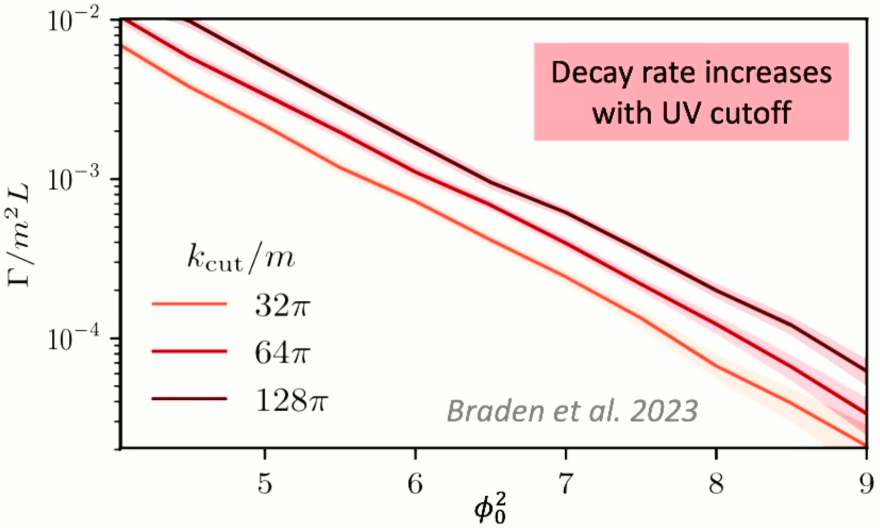

Decay rate increases with UV cutoff

Braden et al. 2023

Discrepancy between lattice results and instanton prediction

Dependence on **UV cutoff**

Possible cause: **renormalization** effects

$$\underbrace{V_{\text{bare}}(\phi)}_{\text{Simulation input}} \neq \underbrace{V_{\text{eff}}(\bar{\phi})}_{\text{Instanton potential}}$$

Probing the effective potential

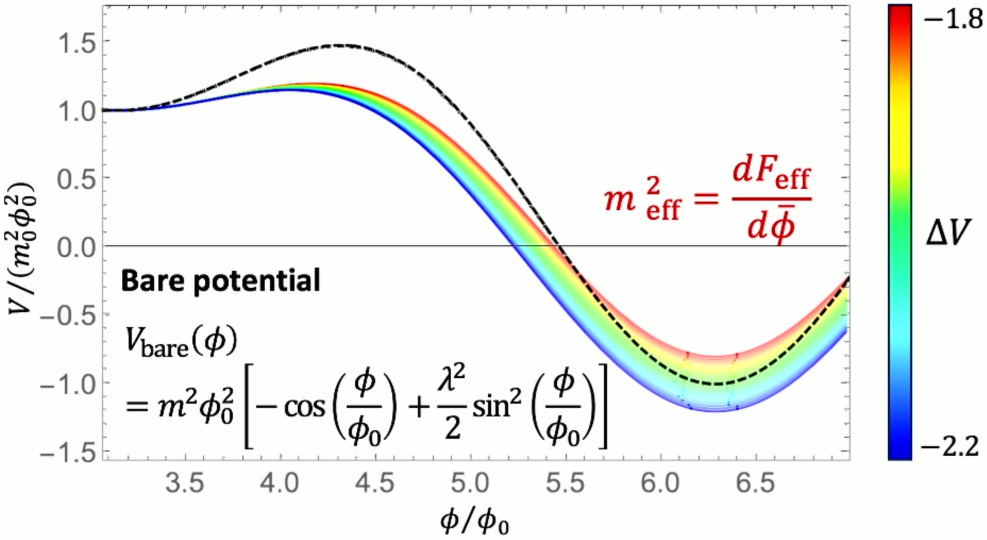

$$m^2_{\text{eff}} = \frac{dF_{\text{eff}}}{d\bar{\phi}}$$

Bare potential

$$V_{\text{bare}}(\phi) = m^2\phi_0^2\left[-\cos\left(\frac{\phi}{\phi_0}\right) + \frac{\lambda^2}{2}\sin^2\left(\frac{\phi}{\phi_0}\right)\right]$$

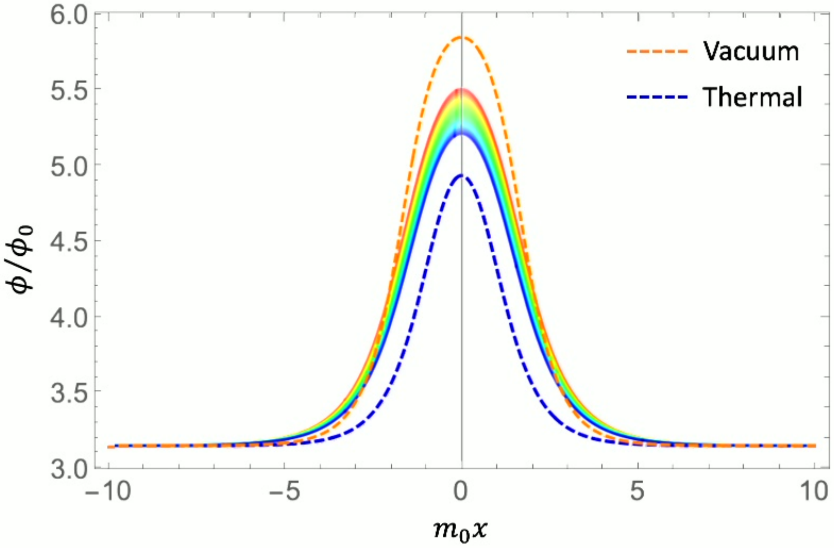

Effective force on $\bar{\phi}$ **in symmetric minima**

$$F_{\text{eff}}(\bar{\phi}) = \langle V'_{\text{bare}}\rangle = \sum_{n=0} \frac{1}{(2n)!} \left.\frac{d^{2n}V'_{\text{bare}}}{d\phi^{2n}}\right|_{\bar{\phi}} \langle \delta\phi^{2n}\rangle$$

- V_{eff} is **not fully determined** in-between the minima!
- **Bubble profiles** are sensitive to the full shape of the potential

Extracting bubble profiles

$$\phi(x,t) = \sum_{k_x k_t} \phi_{k_x k_t} e^{i(k_x x + k_t t)}$$

$$(x_B, t_B) \rightarrow (x', t')$$

$$\phi_B(x_B, t_B) = \sum_{k_x k_t} \phi_{k_x k_t} e^{i(k_x x\prime + k_t t\prime)}$$

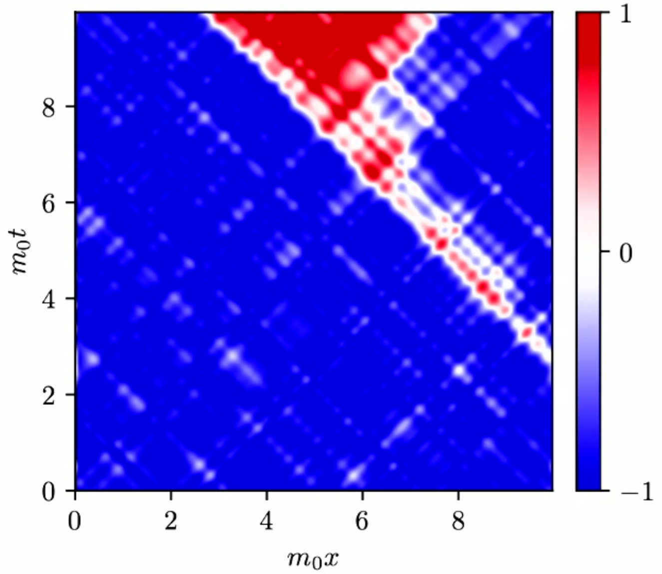

Simulation frame

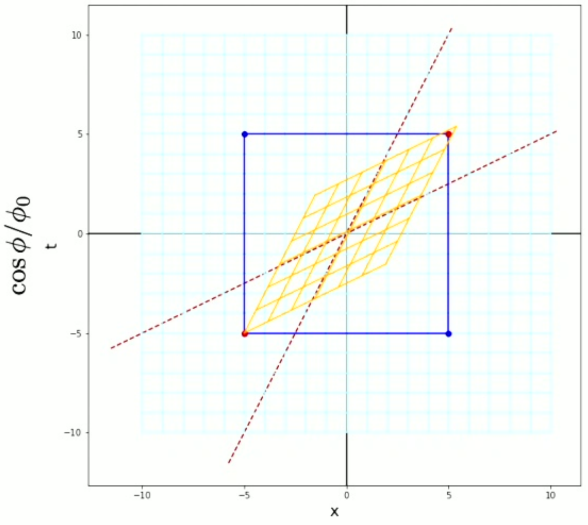

Lorentz transform

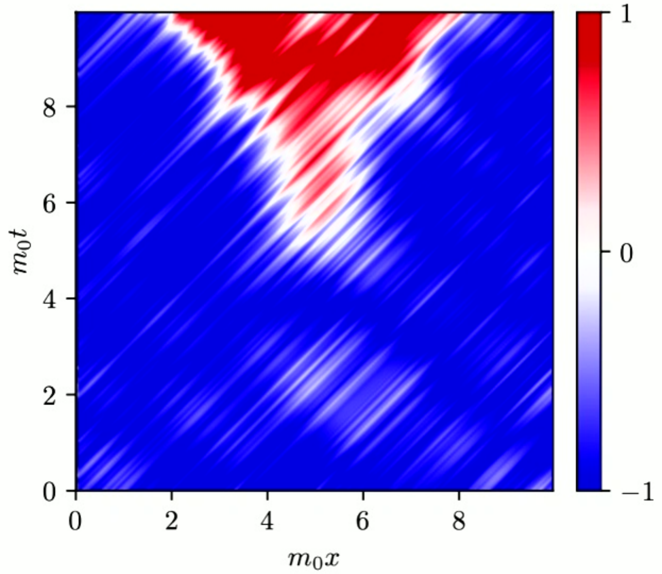

Boosted frame

Extracting bubble profiles

$$\phi(x,t) = \sum_{k_x k_t} \phi_{k_x k_t} e^{i(k_x x + k_t t)}$$

Field profiles around nucleation

$$\phi_B(x_B, t_B) = \sum_{k_x k_t} \phi_{k_x k_t} e^{i(k_x x\prime + k_t t\prime)}$$

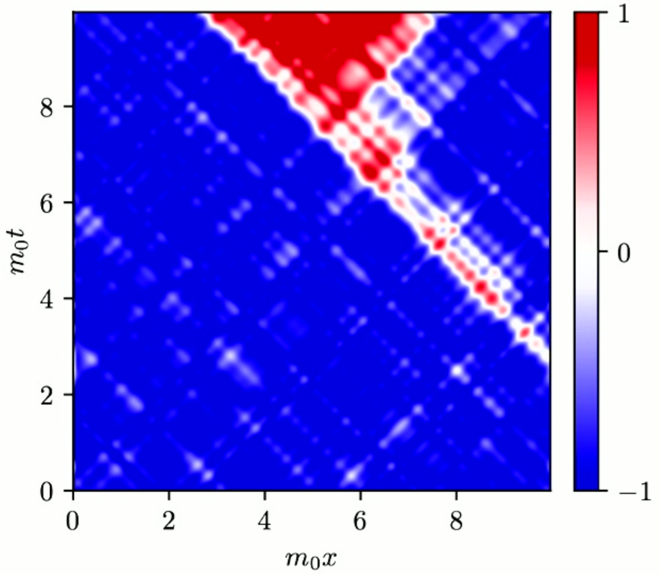

Simulation frame

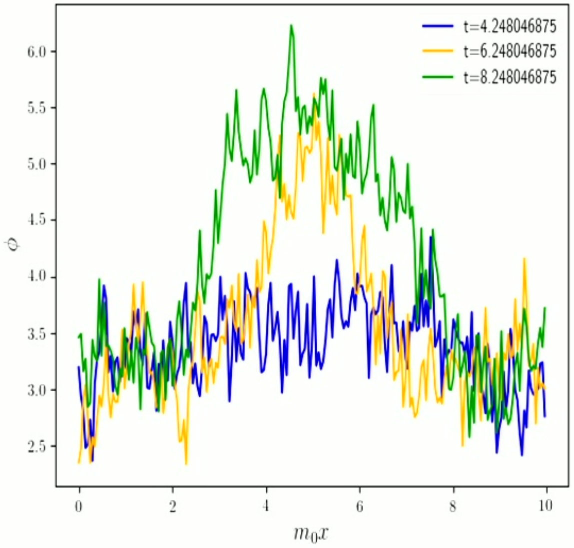

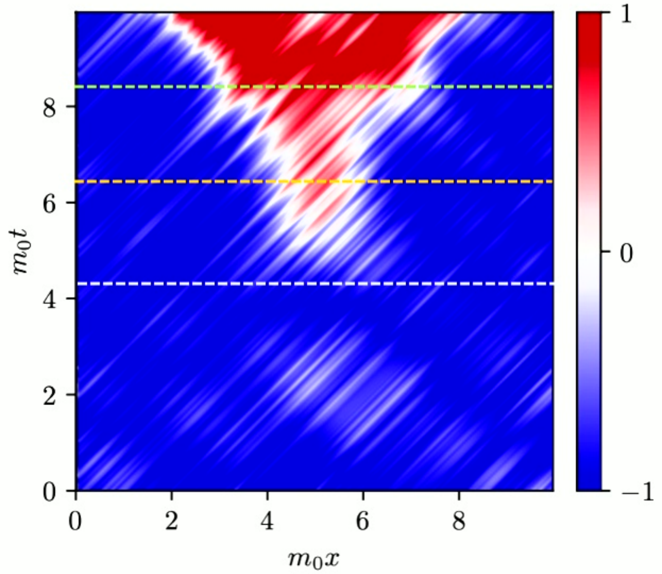

Boosted frame

Outlook: cold-atom analogues

- **BEC** with 2 hyperfine states $\psi_{1,2}(\boldsymbol{x}) = \sqrt{n_{1,2}(\boldsymbol{x})}e^{i\phi_{1,2}(\boldsymbol{x})}$

- **Non-relativistic** Hamiltonian:

$$\hat{H} = \int d\boldsymbol{x} \sum_{i=j}\left[-\hat{\psi}_i^\dagger \frac{\hbar^2}{2m}\nabla^2\hat{\psi}_j + \frac{g}{2}\hat{\psi}_i^\dagger\hat{\psi}_i^\dagger\hat{\psi}_j\hat{\psi}_j\right] - \nu(t)\sum_{i\neq j}\hat{\psi}_i^\dagger\hat{\psi}_j$$

- Low-k EoM for **phase difference** $\hat{\varphi} = \hat{\phi}_1 - \hat{\phi}_2$ is analogue to relativistic scalar field:

$$(c_s^{-2}\partial_t^2 - \nabla^2)\varphi = -V'(\varphi)$$

- For **fast enough** modulation $\nu(t) = \nu_0 + \lambda\hbar\omega\cos(\omega t)$: $\boldsymbol{\varphi \equiv \varphi_{\mathrm{slow}} + \varphi_{\omega}}$ and

$$\boxed{V_{\mathrm{eff}}(\varphi_{\mathrm{slow}}) = V_0\left[-\cos(\varphi_{\mathrm{slow}}) + \frac{\lambda^2}{2}\sin^2(\varphi_{\mathrm{slow}})\right]}$$

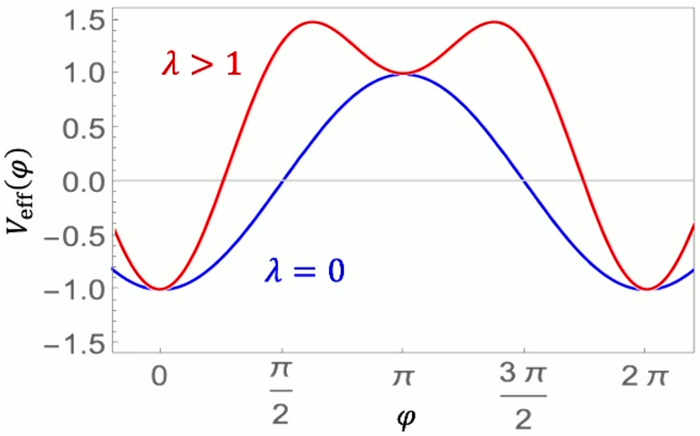

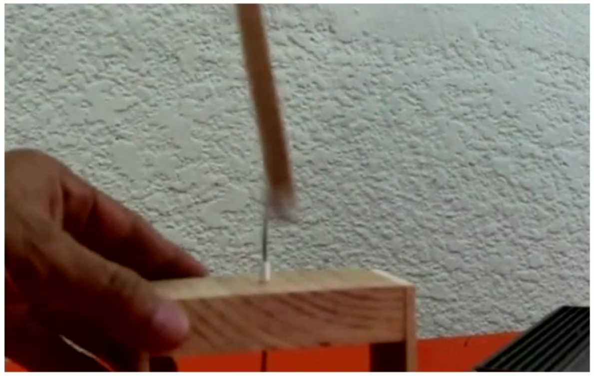

The Big Bang in the lab

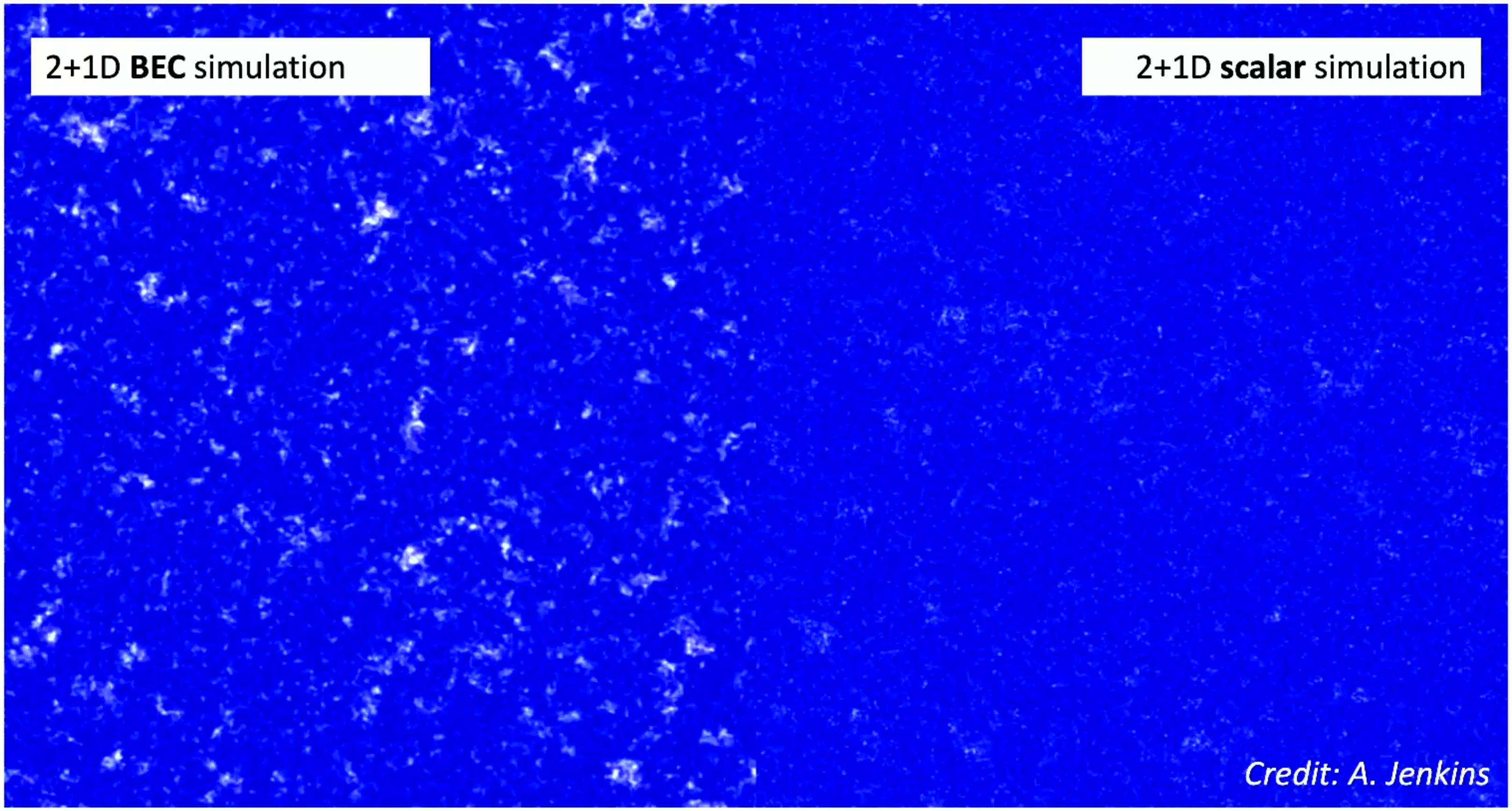

Credit: A. Jenkins

The Big Bang in the lab

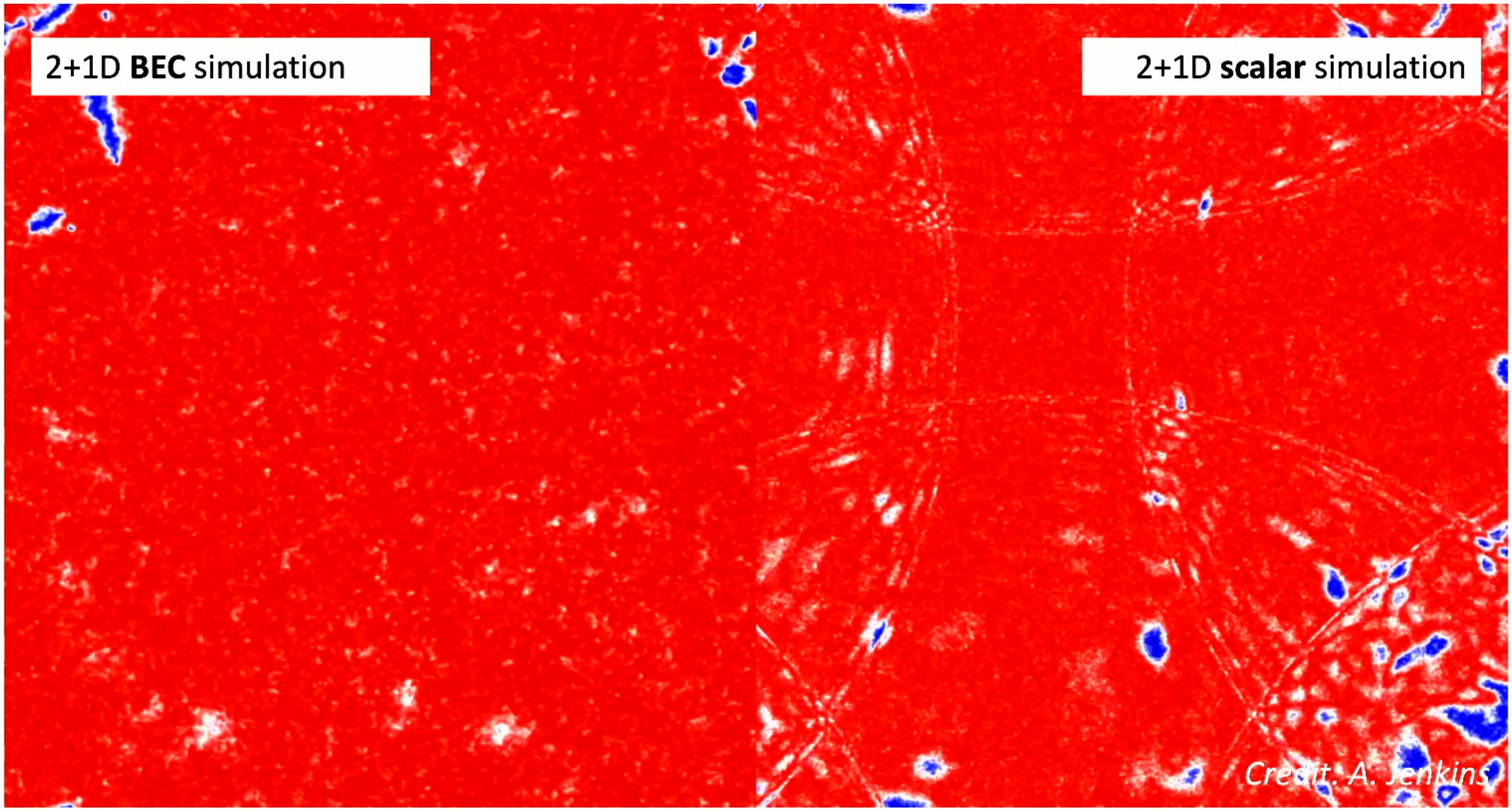

Credit: A. Jenkins

Next steps: quantum simulators

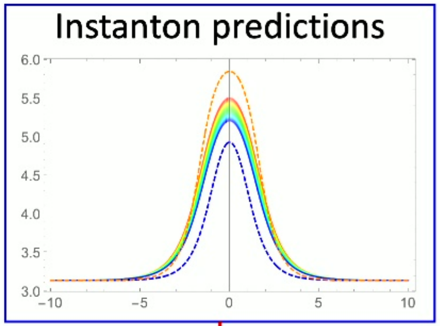

Same decay channels?

Theoretical work on renormalization with **stacked bubble profiles**

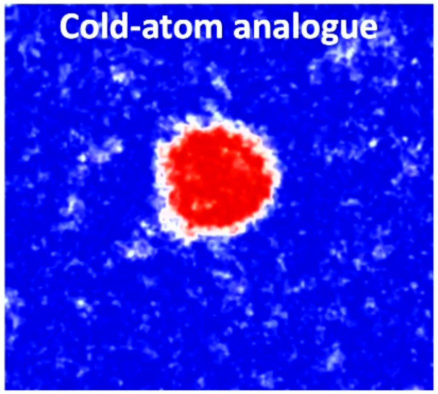

Extend findings to 2 spatial dimensions

Interpretation

- **Range of validity** of lattice approach
- **« Calibration »** in a controlled setting

In progress

March 2025

Next steps: CMB

Delensing for SO Nominal

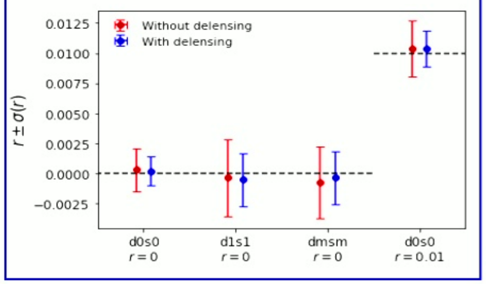

External lensing template

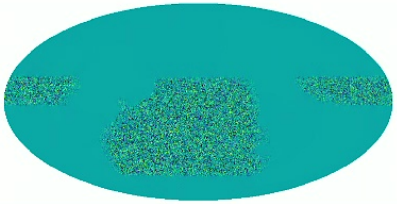

Forecasts with **SO:UK and SO:Japan**

Modelling of **systematics**, e.g. LAT foregrounds

Adapt code to **real data**

First SO *r* report with delensing

Current status

2025

Decreasing noise and $\sigma(r)$

A new perspective on the early Universe

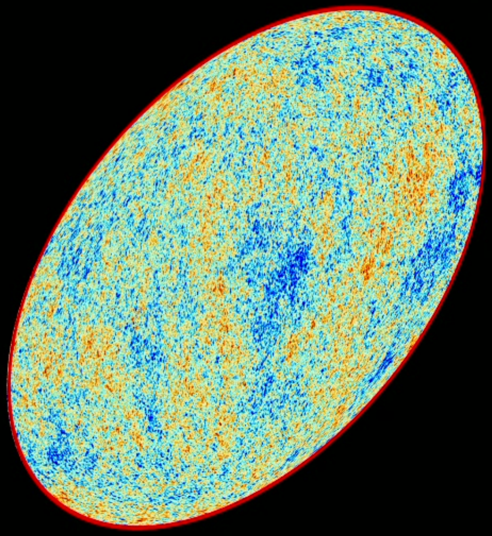

Viable inflationary potentials

- ➢ Favored by data
- ➢ Physically motivated

A new perspective on the early Universe

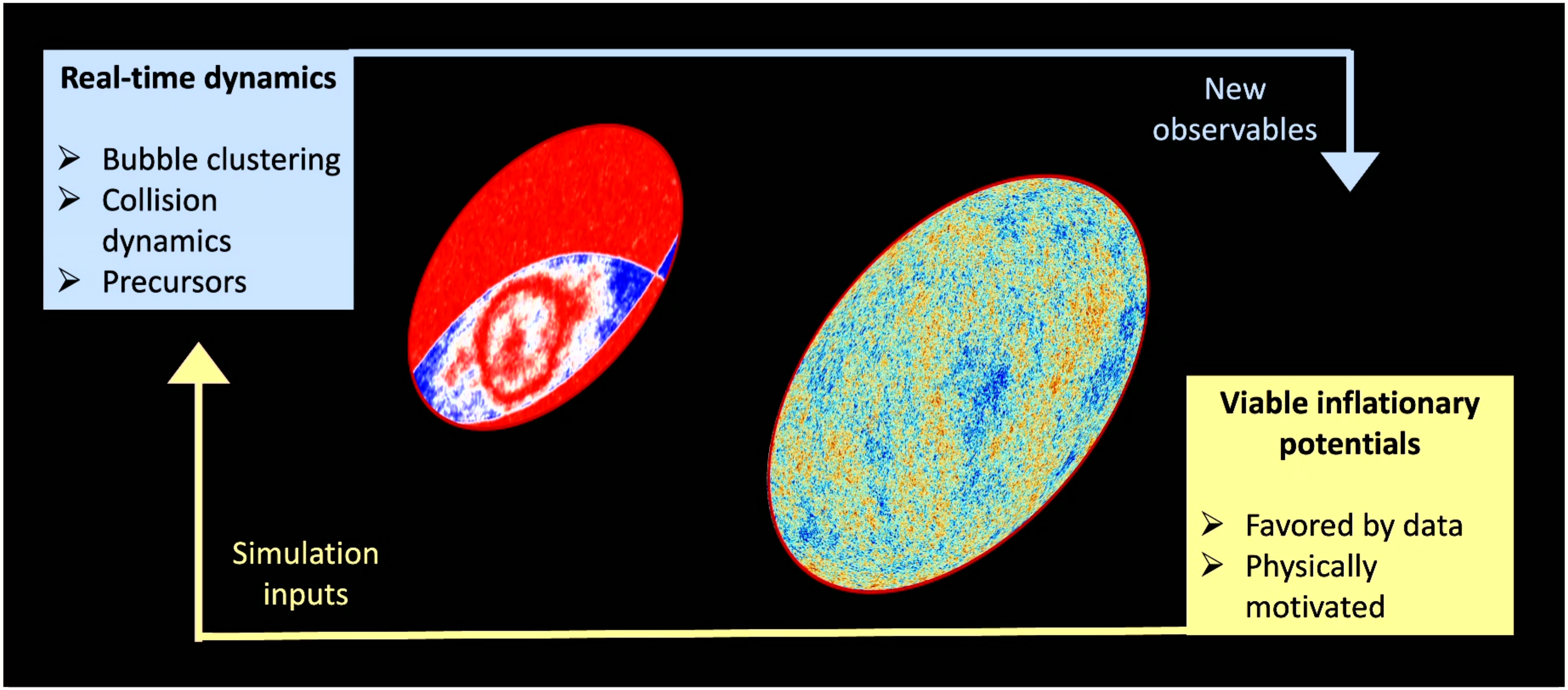

Real-time dynamics

- Bubble clustering
- Collision dynamics
- Precursors

New observables

Viable inflationary potentials

- Favored by data
- Physically motivated

Simulation inputs

A new perspective on the early Universe

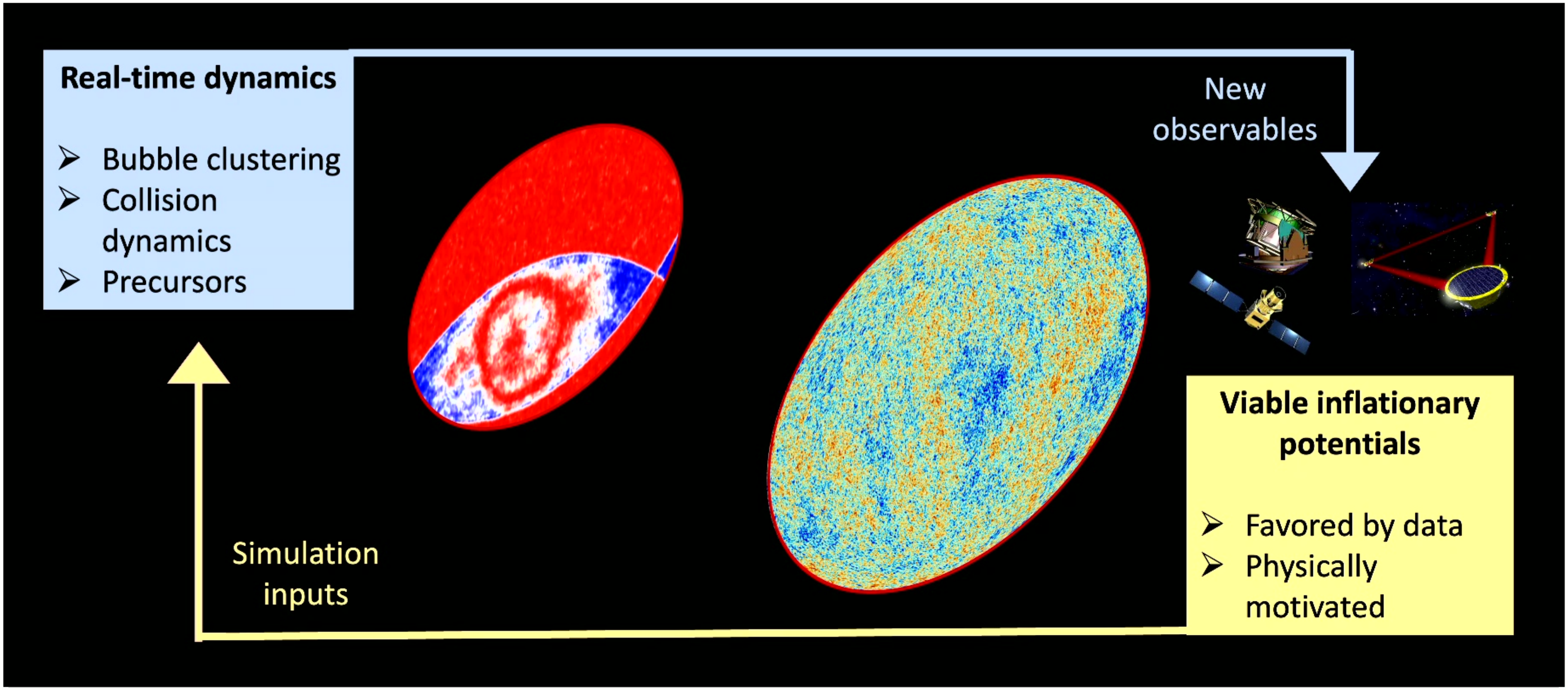

Real-time dynamics

- Bubble clustering
- Collision dynamics
- Precursors

New observables

Viable inflationary potentials

- Favored by data
- Physically motivated

Simulation inputs

The Big Bang in the lab

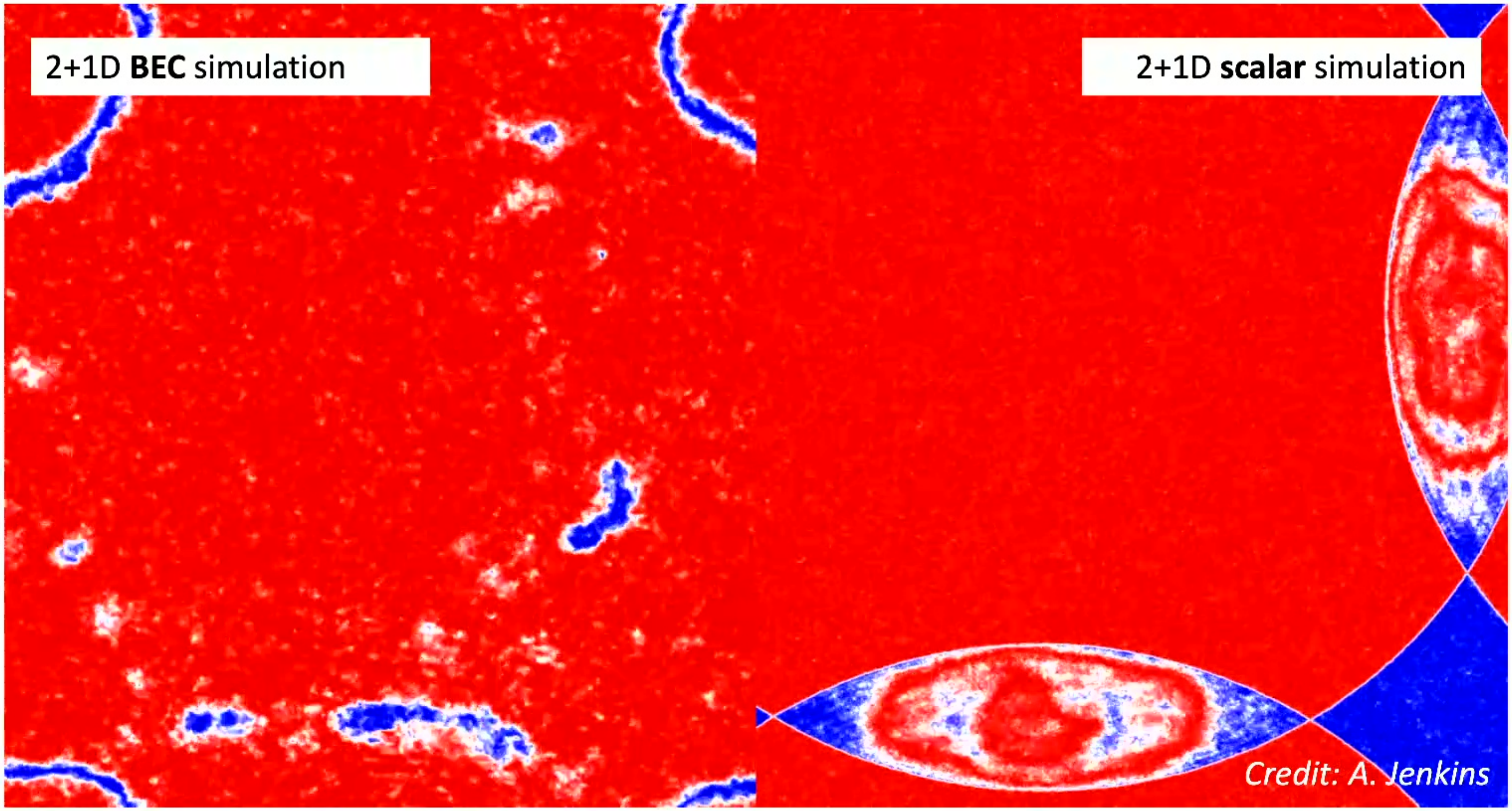

Credit: A. Jenkins